Check for updates

Optimal Control Applications and Methods

WILEY

RESEARCH ARTICLE

Optimal Trajectory Tracking Using Newton and Levenberg-Marquardt-Like Algorithms for Constrained Time-Varying Optimization

Sunidhi Pandey[1] | Parijat Prasun[1] | Shyam Kamal[1] | Devender Singh[1] | Debdas Ghosh[2] | Sorin Olaru[3]

[1]Department of Electrical Engineering, IIT (BHU), Varanasi, India | [2]Department of Mathematical Sciences, IIT (BHU), Varanasi, India | [3]Université Paris-Saclay, CNRS, CentraleSupélec, Laboratoire des Signaux et Systèmes (L2S), 3 Rue Joliot Curie, Gif sur Yvette, France

Correspondence: Sorin Olaru (sorin.olaru@l2s.centralesupelec.fr) | Shyam Kamal (shyamkamal.eee@iitbhu.ac.in)

Received: 27 August 2024 | **Revised:** 19 February 2025 | **Accepted:** 20 March 2025

Funding: The authors received no specific funding for this work.

Keywords: continuous-time optimization | gradient flow | rated convergence | time-varying optimization

ABSTRACT

In this paper, we propose continuous-time algorithms for tracking the optimal trajectory of time-varying optimization problems with time-varying constraints in a predefined time, where the time of convergence is selected a priori. A robust Newton-like approach is developed for the cases, where the exact knowledge of the rate of change of the gradient of objective function is unknown. Levenberg-Marquardt-like algorithm is proposed for the cases when the Hessian of the objective function is singular or near singular. Lyapunov-based convergence analysis is discussed for the proposed algorithms. Simulation results for time-varying optimization problems show the efficacy of the proposed approach. We demonstrate the applicability of the proposed method through its use in a collision-free robot navigation problem.

1 | Introduction

Continuous time optimization algorithms use ordinary differential equations (ODE). In this direction, control theory imparts many mathematical tools to study the convergence of trajectories to their optimal solutions [1]. Most of the studies in the area of optimization techniques are mainly focussed on time-invariant optimization problems. However, in many practical settings, time-varying systems such as overlay traffic engineering problems, drop-off points for drone delivery that are mobile [2], path estimation of a stochastic process [3], computer networks [2], and distributed optimization [4] are examples of time-varying problems.

Solving the time-varying optimization (TVO) problem is equivalent to tracking the optimal trajectory. In TVO, the objective function as well as constraints depend explicitly on time. Information about the dynamics of the TVO problem can be used to anticipate, and further, the gradient/Newton correction to track the optimal trajectory completes the technique. In this regard, few authors [5, 6] studied the variation of prediction-correction ideas in continuous and discrete time, respectively. Rahili and Ren [7] also extended this idea for continuous-time distributed optimization, where convergence to optimal trajectory is asymptotic. Fazlyab et al. [8] utilized the concept of prediction-correction technique to solve TVO problems with time-varying constraints, resulting in asymptotic convergence to the optimal solution.

In recent years, research in the area of TVO has gained a lot of attention due to real-time applications [2, 4], but also from techniques like model predictive control (MPC) which have to

© 2025 John Wiley & Sons Ltd.

guarantee the convergence of an optimization problem in a given amount of time before its reiteration. This has led to a surge in developing techniques that focus on finite/fixed-time convergence of trajectories to the solution of TVO problems [9]. Bhat and Bernstein [10] discussed the concept of finite-time stability (FTS) where the time of convergence to the optimal solution is finite and depends on the initial conditions. Hong et al. [4] explored distributed TVO problems with limited interaction ranges and demonstrated a finite time convergence rate of consensus. Fixed-time stability (FxTS) is a stronger notion than FTS. In FxTS, the upper bound of convergence time is uniform with respect to initial conditions. Hong et al. [9, 11], discussed the fixed-time approach to solve time-varying convex optimization problems.

Many authors [12, 13] studied a subclass of FxTS called a predefined/prescribed upper bound of settling time (PUBST) based stability, where the upper bound of convergence time can be chosen in advance irrespective of initial conditions. Pal et al. [14] studied a distinctive notion of PUBST-based stability. Prasun et al. [15] also discussed the concept of PUBST related to gradient-flow systems. Furthermore, many authors have also discussed the notion of PUBST (see, e.g., [16, 17]) with respect to the various applications.

In this paper, a prediction-correction approach is employed to track the optimizer trajectories of TVO problems. Fazlab et al. [8] studied the prediction–correction-based continuous time dynamical system technique to solve constrained TVO problems and guarantee the asymptotic convergence of proposed dynamics to optimal solutions. Later, Hong et al. [9] extended this approach by proposing continuous time dynamics to solve TVO problems with equality constraints in fixed time. In this paper, utilizing the concept of PUBST-based convergence where bound on convergence time can be chosen a priori, we modified the prediction-correction-based continuous time dynamics to solve constrained TVO problems with PUBST-based convergence to the optimal trajectory. To the best of the authors' knowledge, this paper is the first to study PUBST-based continuous time dynamics to solve constrained TVO problems, in addition to discussion for modification in the dynamics when exact information about the time rate of change of the gradient of the objective function is unknown and cases when Hessian of the objective function is not invertible. The main contributions of this paper are as follows:

(A) Newton-like PUBST-based stable dynamics is proposed to solve TVO problems and its Lyapunov-based convergence analysis is discussed for both unconstrained as well as constrained case.

(B) A robust Newton-like PUBST-based stable dynamics is proposed for the cases when we do not have the exact knowledge of the time derivative of the gradient of the objective function.

(C) Levenberg-Marquardt-like PUBST-based stable dynamics is proposed for the cases when the Hessian of the objective function is not invertible with the assumption of gradient dominance. The convergence analysis of this dynamics is studied in the sense of input-to-state stability (ISS), where the input is a perturbation from the true Hessian.

(D) Numerical examples for unconstrained case and constrained case of TVO problems are demonstrated using the proposed method. We have also shown that the discretized implementation is conterminous with theoretical results.

(E) We demonstrate the application of the proposed approach in robot navigation with collision avoidance. We explore situation where the robot is tasked with tracking a moving target in a priori chosen time.

This note is structured as follows. Section 2 is dedicated to notations and preliminaries. In Section 3, problem statement is discussed. Section 4 presents the main result for unconstrained time-varying optimization problems. In Section 4.2, the results discussed in Section 4 are extended for constrained TVO. Numerical examples are illustrated in Section 5 based on the results discussed in Sections 4 and 4.2. Finally, the conclusion ends the paper.

2 | Notations and Preliminaries

2.1 | Notations

$\mathbb{R}, \mathbb{R}_{\geq 0}$ and $\mathbb{R}^m$ be the fields of real numbers, nonnegative numbers and m dimensional Euclidean space, respectively. $\|\cdot\|$ denotes Euclidean norm. max denotes the greatest element of the set. $(\cdot)^\top$ refers to the transpose. A time-varying objective function is defined as $f(t,x)$ then $\nabla f : \mathbb{R}_{\geq 0} \times \mathbb{R}^n \to \mathbb{R}^n$ and $\nabla^2 f : \mathbb{R}_{\geq 0} \times \mathbb{R}^n \to \mathbb{R}^{n \times n}$ denotes the gradient and Hessian of function $f : \mathbb{R}_{\geq 0} \times \mathbb{R}^n \to \mathbb{R}$ with respect to $x \in \mathbb{R}^n$. I_n is an identity matrix of dimension n. A function $\kappa : \mathbb{R}_{\geq 0} \to \mathbb{R}_{\geq 0}$ belongs to class $\mathcal{K}$, if it is strictly increasing and continuous with $\kappa(0) = 0$. Additionally, if a class $\mathcal{K}$ function does not saturate meaning $\kappa(x) \to \infty$, as $x \to \infty$, then it belongs to class $\mathcal{K}_\infty$. If a function $\kappa : \mathbb{R}_{\geq 0} \to \mathbb{R}_{\geq 0}$ is continuous with $\kappa(0) = 0$ and satisfies $\begin{cases} \kappa(x_1) > \kappa(x_2), & \text{if } \kappa(x_1) > 0, x_1 > x_2 \\ \kappa(x_1) = \kappa(x_2), & \text{if } \kappa(x_1) = 0, x_1 > x_2, \end{cases}$ belongs to generalized $\mathcal{K}$ ($\mathcal{GK}$) function. A function $\phi : \mathbb{R}_{\geq 0} \times \mathbb{R}_{\geq 0} \to \mathbb{R}_{\geq 0}$ belongs to generalized $\mathcal{KL}$ ($\mathcal{GKL}$) class functions if for each fixed $t \geq 0$ the function $\phi(s,t)$ is a $\mathcal{GK}$ function and for every fixed $s \geq 0$, the function $\phi(s,t)$ is continuous, and goes to zero as $t \to \mathcal{T}$ for some $\mathcal{T} \leq \infty$. Next, if $\mathcal{T}$ can be chosen arbitrarily, then ϕ is called arbitrary $\mathcal{GKL}$ ($\mathcal{AGKL}$) class functions.

2.2 | PUBST-Based Stability

Consider the following system

$$\dot{z} = \mathcal{G}(t, z, \varrho), \quad z(t_0) = z_0 \tag{1}$$

where $z \in D \subset \mathbb{R}^n$, t_0 is the initial time, $\varrho \in \mathbb{R}^q$ is the vector of system parameters to be tuned and $\mathcal{G} : \mathbb{R}_{\geq 0} \times D \times \mathbb{R}^q \to \mathbb{R}^n$ is continuous vector field such $\mathcal{G}(t, 0, \varrho) = 0$, $\forall t \geq 0$ that is $z = 0$ is an equilibrium point of (1).

Remark 1. In this paper, we use the notions of stability in accordance with arbitrary time convergence [14] and to maintain uniformity with the notions present in existing literature, this paper uses the terminology: Predefined upper bound of settling time (PUBST) based stability instead of arbitrary time stability.

1099154, 2025, 4, Downloaded from https://onlinelibrary.wiley.com/doi/10.1002/oca.3292 by Indian Institute Of Technology, Wiley Online Library on [05/06/2026]. See the Terms and Conditions (https://onlinelibrary.wiley.com/terms-and-conditions) on Wiley Online Library for rules of use; OA articles are governed by the applicable Creative Commons License

Definition 1 ([14] PUBST-based stable). The zero solution of the non-autonomous system (1) is called PUBST-based stable

- It is asymptotically stable and additionally trajectories $z(t, t_0, z_0)$ of (1) converges to the origin in some finite time and $z = 0$ is maintained $\forall\ t \geq t_0 + T(t_0, z_0)$, where $T : \mathbb{R}_{\geq 0} \times D \rightarrow \mathbb{R}_{\geq 0}$ is the settling time,
- $\exists$ a PUBST duration T_r, which does not depend on any initial conditions and can be chosen a priori and $t_f := T_r + t_0$, where t_f is PUBST for convergence.

Remark 2. The condition $T_r \geq T_{ac}$ (weak PUBST stable) follows $\forall z_0 \in D$, where T_{ac} is the actual duration from t_0 within which solutions converge.

Remark 3. It is important to note that t_f does not depend explicitly on any system parameters, t_f is an independent parameter that is chosen in advance. Theoretically, t_f can be chosen as any arbitrarily small value but inherent dynamics of practical systems (specifically actuator dynamics) impose restrictions on choosing arbitrarily small values of t_f.

Lemma 1 ([14]). *Consider the system (1). Let $D \subset \mathbb{R}^n$ contain $z = 0$ and $\gamma_1(z)$ and $\gamma_2(z)$ be continuous positive definite functions. Assume that there exists a continuously differentiable scalar function $\mathcal{V} : I \times D \rightarrow \mathbb{R}_{\geq 0}$, $(I = [t_0, \infty))$ and $\vartheta > 1$ such that*

- $\gamma_1(z) \leq \mathcal{V}(t, z) \leq \gamma_2(z), \forall z \in D \setminus \{0\}, \forall t \in [t_0, \infty)$
- $\mathcal{V}(t, 0) = 0, \forall t \in I$
- *For* $\mathcal{V} \neq 0$, $\frac{d}{dt}\mathcal{V}(t, z) \leq \begin{cases} \frac{-\vartheta(e^{\mathcal{V}(t,z)}-1)}{e^{\mathcal{V}(t,z)}(t_f - t)}, & \text{if} \quad t_0 \leq t < t_f \\ 0, & \text{otherwise.} \end{cases}$

Then the origin of system (1) is PUBST-based stable.

Note that PUBST-based stability of $z = 0$ is for any $\epsilon > 0$, there exists, $t_f > 0$ such that $z(t) < \epsilon, \forall t \geq t_f$ and $\forall t_0 \geq 0$.

Remark 4. Note that T_r is an independent parameter itself, which is chosen in advance. Theoretically, T_r can be chosen arbitrarily small but due to practical limitations, it is suitable to avoid such stringent requirements.

Existence and uniqueness of the solution: Let us consider the following system [14]

$$\dot{z} = u; \quad z \in \mathbb{R}_{\geq 0} \tag{2}$$

$$u = \begin{cases} -\frac{\vartheta(e^z - 1)}{e^z(t_f - t)} & \text{if } t_0 \leq t < t_f \\ 0, & \text{otherwise} \end{cases} \tag{3}$$

with $z(t_0)$ as the initial condition. The solution to (2) is: $z = \ln\left(1 + \chi\left(t_f - t\right)^{\vartheta}\right)$, where $\chi = \frac{e^{z(t_0)}-1}{(t_f - t_0)^{\vartheta}} \geq 0$, By substituting this solution in (3), we get,

$$u = \begin{cases} \frac{-\vartheta\left(\chi\left(t_f - t\right)^{\vartheta - 1}\right)}{\left(1 + \chi\left(t_f - t\right)^{\vartheta}\right)}, & \text{if } t_0 \leq t < t_f \\ 0, & \text{otherwise} \end{cases} \tag{4}$$

From (4), for $\chi \geq 1, |u| < \vartheta\chi, \forall t \geq t_0$ and for $\chi < 1, |u| \leq \vartheta, \forall t \geq t_0$, Hence, u is continuous in z, $\forall$ fixed t, while measurable in t, $\forall$ fixed z and bounded by a quantity that is integrable over a finite-time interval. So, for $t < t_f$, all the conditions for the existence of solution are satisfied for (2) in Carathéodory sense, therefore, a solution is extended till t_f. For $t > t_f$, a classical solution exists, and hence, we can say that the solution exists for $[t_0, \infty)$. The above analysis is same as when solutions are analyzed in the sense of Filippov for differential equations with discontinuous right-hand side [18]. Hence, the existence and uniqueness of the solution are established for the PUBST algorithm.

2.3 | PUBST-Based Input-To-State Stability (PUBST-ISS)

Consider the following non-autonomous system

$$\dot{z} = \mathcal{G}(t, z, d), \ t \geq t_0, \ z \in \mathbb{R}^n, \ d \in \mathbb{R}^m \tag{5}$$

where $\mathcal{G}$ is continuous in (t, z, d) and $\mathcal{G}(t, 0, 0) = 0$.

Definition 2 ([19]). A continuous function $\mathcal{V}(t, z)$ is said to be PUBST-ISS Lyapunov function for (5) if (a) $\exists\ \mathcal{K}_\infty$ functions α_1 and α_2 such that $\alpha_1(\|z\|) \leq \mathcal{V}(t, z) \leq \alpha_2(\|z\|)\ \forall z \in \mathbb{R}^n$ (b) $\exists$ class $\mathcal{K}$ functions α_3 and α_4 and $\mathcal{AGKL}$ class function β for any solution $z(t)$ of the system (5) such that $\|z(t)\| \geq \alpha_4(\|d\|) \Rightarrow \dot{\mathcal{V}}(t, z) \leq -\beta(\|z_0\|, t_f - t) - \alpha_3(\|z\|)\ \forall t \geq 0$, and $\beta(\|z_0\|, t_f - t) \mapsto \vartheta\frac{e^{\mathcal{V}}-1}{e^{\mathcal{V}}(t_f - t)}$, $\alpha_3(\|z\|) \mapsto \vartheta_2\mathcal{V}^\alpha$, where $\vartheta > 1, \vartheta_2 > 0, \alpha > 0, t_f > t \geq 0$.

Lemma 2 ([19]). *System (5) is PUBST-ISS if it admits a PUBST-ISS Lyapunov function.*

3 | Problem Statement

Consider the following Time Varying Optimization (TVO) problem

$$\begin{aligned} z^*(t) := \ & \underset{z \in \mathbb{R}^n}{\operatorname{argmin}}\ \mathcal{F}(t, z) \\ & \text{subject to} \quad g_i(t, z) \leq 0, \quad i \in \{1, 2, \ldots, r\} \end{aligned} \tag{6}$$

where $\mathcal{F} : \mathbb{R}_{\geq 0} \times \mathbb{R}^n \rightarrow \mathbb{R}$, $g = [g_1, g_2, \ldots, g_r]^\top$ with all g_i being convex functions in $z \in \mathbb{R}^n, \forall t \geq 0$ and fulfills following Assumptions.

Assumption 1.

1. The objective function $\mathcal{F} : \mathbb{R}_{\geq 0} \times \mathbb{R}^n \rightarrow \mathbb{R}$ is twice continuously differentiable with respect to z, continuously differentiable with respect to t, and convex with respect to z.
2. A unique optimal solution $z^*(t)$ exists.

Assumption 2 (Polyak-Łojasiewicz inequality [20]).

$$w(\mathcal{F}(t, z) - \mathcal{F}^*(t))^p \leq \|\nabla\mathcal{F}(t, z)\| \tag{7}$$

where $\mathcal{F}^* := \min_{z \in \mathbb{R}^n} \mathcal{F}(t, z), 0 < p < 1$ and $w > 0$.

10991514, 2025, 4, Downloaded from https://onlinelibrary.wiley.com/doi/10.1002/oca.3292 by Indian Institute Of Technology, Wiley Online Library on [05/06/2026]. See the Terms and Conditions (https://onlinelibrary.wiley.com/terms-and-conditions) on Wiley Online Library for rules of use; OA articles are governed by the applicable Creative Commons License

Assumption 3. The inequality constraint functions $g_i(t,z)$ are twice continuously differentiable with respect to z and continuously differentiable with respect to t.

Assumption 4 (Constraint Qualification). There exists atleast one $z(t) \in \mathbb{R}^n$ such that $g_i(t,z) < 0$, $\forall i \in \{1,2,\ldots r\}$ and $\forall t \geq 0$.

Remark 5. For TVO problem (8), Assumption 1 is an important condition for the convergence of gradient-based methods to an optimal solution [21]. In Karimi et al. [20], it is noted that Assumption 2 is the weakest condition among similar conditions commonly used in the literature to demonstrate convergence in gradient-based algorithms.

Consider the following unconstrained Time Varying Optimization (TVO) problem

$$z^*(t) := \underset{z\in\mathbb{R}^n}{\operatorname{argmin}}\ \mathcal{F}(t,z) \tag{8}$$

Lemma 3 ([21]). *The continuously differentiable convex function $\mathcal{F} : \mathbb{R}_{\geq 0} \times \mathbb{R}^p \to \mathbb{R}$ is minimized at solution $s^*(t)$ if and only if $\nabla\mathcal{F}(t,s^*) = 0, \forall t$.*

The optimal trajectory $z^*(t)$ satisfies the first-order optimality condition $\nabla\mathcal{F}(t,z^*) = 0$, $\forall t \geq 0$, then time derivative of this condition will also be zero which results in $\nabla^2\mathcal{F}(t,z)\dot{z}^*(t) + \frac{\partial\nabla\mathcal{F}(t,z)}{\partial t} = 0$. Solving for $\dot{z}^*(t)$ leads to following dynamical system:

$$\dot{z}^*(t) = -\nabla^2\mathcal{F}(t,z)^{-1}\frac{\partial\nabla\mathcal{F}(t,z)}{\partial t} \tag{9}$$

If the optimal solution $z^*(t)$ was known for some $t_0 > 0$, the system in (9) could be used to track the evolution of $z^*(t)$. As we do not have access to $z^*(t)$ at any point in time, we propose PUBST-based algorithms to solve TVO problem in a priori chosen time utilizing the idea of prediction and correction.

4 | Main Results

Here, we discuss PUBST convergent dynamics to solve TVO problems. The main result of this note discusses TVO problems for which $\lim_{t\to t_f}\|z(t) - z^*(t)\| = 0$, where $t_f < \infty$, that is chosen a priori. The convergence of the trajectories based on the PUBST algorithm to the optimal solution $z^*(t)$ also signifies $\lim_{t\to t_f}\|\nabla\mathcal{F}(t,z)\| = 0$. First, we consider TVO problems (8), where $\mathcal{F}(t,z)$ is given so $\nabla\mathcal{F}(t,z)$ is known $\forall t$, and aim is to converge to optimal solution $z^*(t)$ within priori chosen time t_f.

4.1 | Predefined Upper Bound of Settling Time-Based Convergent Dynamics for Time-Varying Optimization (PUBSTC-TVO)

In this subsection, we present two PUBST-based dynamical systems to solve unconstrained TVO problems as (8). One is based on the assumption that $\nabla^2\mathcal{F}$ is invertible and second if we do not consider $\nabla^2\mathcal{F}$ to be invertible. We revise Equation (9) by adding a correction term to propose dynamics that track the optimal trajectory in a predefined time.

4.1.1 | Newton-Like PUBSTC-TVO

Let $\nabla^2\mathcal{F}$ is invertible then in order to track $z^*(t)$ of (8) in PUBST, we propose the following dynamics

$$\dot{z}(t) = \begin{cases} -(\nabla^2\mathcal{F}(t,z))^{-1}\left(\vartheta\psi(t,z) + \frac{\partial\nabla\mathcal{F}(t,z)}{\partial t}\right), & \text{for } t_0 \leq t < t_f \\ -(\nabla^2\mathcal{F}(t,z))^{-1}\left(\vartheta\nabla\mathcal{F}(t,z) + \frac{\partial\nabla\mathcal{F}(t,z)}{\partial t}\right), & \text{for } \quad t \geq t_f \end{cases} \tag{10}$$

where $z(t) \in \mathbb{R}^n$, $\vartheta \in \mathbb{R}$ and satisfies $\vartheta > 1$, $\psi(t,z) = (\psi_1,\psi_2,\ldots,\psi_n) \in \mathbb{R}^{n\times 1}$, $\psi_i = \frac{(e^{\nabla\mathcal{F}_{z_i}(t,z)}-1)}{e^{\nabla\mathcal{F}_{z_i}(t,z)}(t_f-t)}$, for $1 \leq i \leq n$.

Theorem 1. *Consider the dynamics (10). Suppose that $\mathcal{F} : \mathbb{R}_{\geq 0} \times \mathbb{R}^n \to \mathbb{R}$ in (8) has invertible Hessian, satisfies Assumption 1, and there exist a continuously differentiable function $V : [t_0,\infty) \times \mathbb{R}^n \to \mathbb{R}$, satisfying $\gamma_1(z) \leq V(t,z) \leq \gamma_2(z)$, $\forall z \in \mathbb{R}^n \setminus \{0\}, \forall t \in [t_0,\infty)$, $\gamma_1(z)$ and $\gamma_2(z)$ be continuous positive definite functions, $V(t,z^*) = 0$ and for $V \neq 0$: $\dot{V} \leq 0, \forall t \geq t_f$ and $\dot{V} \leq \frac{-\vartheta(e^V-1)}{e^V(t_f-t)}, \forall t \in [t_0,t_f)$ for (10), then the equilibrium point of dynamics (10) is PUBST-based stable. This also signifies that $z(t)$ converges to the optimal solution $z^*(t)$ in a priori chosen time.*

Proof. Let us select the Lyapunov function candidate

$$V = \|\nabla\mathcal{F}(t,z)\|^2 \tag{11}$$

The derivative of the V along the dynamics (10) for $t \in [t_0,t_f)$

$$\begin{aligned}\dot{V}(z) &= 2(\nabla\mathcal{F}(t,z))^\top\left(\nabla^2\mathcal{F}(t,z)\dot{z} + \frac{\partial\nabla\mathcal{F}(t,z)}{\partial t}\right)\\ &= 2\nabla\mathcal{F}^\top\left(\nabla^2\mathcal{F}\left(-(\nabla^2\mathcal{F})^{-1}\left(\vartheta\psi + \frac{\partial\nabla\mathcal{F}}{\partial t}\right)\right) + \frac{\partial\nabla\mathcal{F}}{\partial t}\right)\\ &= -2\vartheta(\nabla\mathcal{F}(t,z))^\top\psi(t,z)\end{aligned} \tag{12}$$

$$\begin{aligned}&\leq -2\vartheta(\nabla\mathcal{F}_{z_i}(t,z))\psi_i(t,z) \qquad \text{for any i}\\ &\leq -2\vartheta\frac{|\nabla\mathcal{F}_{z_i}(t,z)|(e^{|\nabla\mathcal{F}_{z_i}(t,z)|}-1)}{e^{|\nabla\mathcal{F}_{z_i}(t,z)|}(t_f-t)}\end{aligned} \tag{13}$$

Since, $V \leq n(\max\{|\nabla\mathcal{F}_1|,|\nabla\mathcal{F}_2|,\ldots,|\nabla\mathcal{F}_n|\}^2)$ and thus, $\sqrt{V/n} \leq \max\{|\nabla\mathcal{F}_1|,|\nabla\mathcal{F}_2|,\ldots,|\nabla\mathcal{F}_n|\}$. We assume that at a particular time, $\max\{|\nabla\mathcal{F}_1|,|\nabla\mathcal{F}_2|,\ldots,|\nabla\mathcal{F}_n|\}$ returns $|\nabla\mathcal{F}_i|$, then, $\sqrt{V/n} \leq |\nabla\mathcal{F}_i|$. Using this fact in (13)

$$\dot{V}(z) \leq -2\vartheta\frac{\sqrt{V/n}(e^{\sqrt{V/n}}-1)}{e^{\sqrt{V/n}}(t_f-t)} \tag{14}$$

Let $\hat{V} = \sqrt{V/n}$, hence, $\dot{\hat{V}} = \frac{\dot{V}}{2n\hat{V}}$, so (14) is simplified and yields,

$$\dot{\hat{V}} \leq -\frac{\hat{\vartheta}(e^{\hat{V}}-1)}{e^{\hat{V}}(t_f-t)} \tag{15}$$

where $\hat{\vartheta} = \frac{\vartheta}{n} > 1$. Thus, inequality (15) represents PUBST based stability according to Lemma 1, which means that $\|\nabla\mathcal{F}(t,z)\| \to 0$ as $t \to t_f$, leading to the convergence of trajectory of (10) to the

10991514, 2025, 4, Downloaded from https://onlinelibrary.wiley.com/doi/10.1002/oca.3292 by Indian Institute Of Technology, Wiley Online Library on [05/06/2026]. See the Terms and Conditions (https://onlinelibrary.wiley.com/terms-and-conditions) on Wiley Online Library for rules of use; OA articles are governed by the applicable Creative Commons License

optimal solution $z^*(t)$ of $\mathcal{F}(t,z)$ in a priori chosen time. Next, the time derivative of the V along (10) for $t \geq t_f$ gives

$$\begin{aligned}\dot{V}(z) &= 2(\nabla\mathcal{F}(t,z))^\top\left(\nabla^2\mathcal{F}(t,z)\dot{z} + \frac{\partial\nabla\mathcal{F}(t,z)}{\partial t}\right)\\ &= 2\nabla\mathcal{F}^\top\left(\nabla^2\mathcal{F}\left(-(\nabla^2\mathcal{F})^{-1}\left(\vartheta\nabla\mathcal{F} + \frac{\partial\nabla\mathcal{F}}{\partial t}\right)\right) + \frac{\partial\nabla\mathcal{F}}{\partial t}\right)\\ &= -2\vartheta(\nabla\mathcal{F}(t,z))^\top\nabla\mathcal{F}(t,z)\\ &= -2\vartheta||\nabla\mathcal{F}(t,z)||^2\\ &= -2\vartheta V\end{aligned}$$

So, for $t \geq t_f$, the equilibrium point of system (10) is asymptotically stable, therefore trajectories of (10) will maintain $z^*(t)$. Hence, the equilibrium point of dynamics (10) is PUBST-based stable. □

Remark 6. Contrary to the iterative Newton method, continuous-time flow doesn't inherently demonstrate a quicker convergence rate relative to other gradient flows. With the inverted Hessian metric, convergence maintains isotropy, meaning it occurs uniformly from all directions. This characteristic effectively mitigates the challenges posed by the ill-conditioning of the objective function [22].

Remark 7. In (10), it is required to know the true information of $\frac{\partial\nabla\mathcal{F}(t,z)}{\partial t}$.

4.1.2 | Robust Newton-Like PUBSTC-TVO

In the previous subsection, we require the exact knowledge of $\frac{\partial\nabla\mathcal{F}(t,z)}{\partial t}$. Here, we assume that $\frac{\partial\nabla\mathcal{F}(t,z)}{\partial t}$ is unknown, but $\exists\ell \in \mathbb{R}_{>0}$ such that $\left\|\frac{\partial\nabla\mathcal{F}(t,z)}{\partial t}\right\| \leq \ell$, then in order to track $z^*(t)$ of (8) in PUBST, we propose the following dynamics

$$\dot{z}(t) = \begin{cases} -(\nabla^2\mathcal{F}(t,z))^{-1}\left(\vartheta\psi(t,z) + \ell\frac{\nabla\mathcal{F}(t,z)}{\|\nabla\mathcal{F}(t,z)\|}\right), & t_0 \leq t < t_f\\ -(\nabla^2\mathcal{F}(t,z))^{-1}\left(\vartheta\nabla\mathcal{F}(t,z) + \ell\frac{\nabla\mathcal{F}(t,z)}{\|\nabla\mathcal{F}(t,z)\|}\right), & t \geq t_f\end{cases} \tag{16}$$

where $z(t) \in \mathbb{R}^n$, $\vartheta \in \mathbb{R}$ and satisfies $\vartheta > 1$, $\psi(t,z) = (\psi_1, \psi_2, \dots, \psi_n) \in \mathbb{R}^{n\times 1}$, $\psi_i = \frac{(e^{\nabla\mathcal{F}_{z_i}(t,z)}-1)}{e^{\nabla\mathcal{F}_{z_i}(t,z)}(t_f-t)}$, for $1 \leq i \leq n$.

Theorem 2. *Consider the dynamics (16). Suppose that $\mathcal{F}: \mathbb{R}_{\geq 0}\times\mathbb{R}^n \to \mathbb{R}$ in (8) has invertible Hessian with $\left\|\frac{\partial\nabla\mathcal{F}}{\partial t}\right\| \leq \ell$, $\ell \in \mathbb{R}_{>0}$ satisfies Assumption 1 and $\exists$ a continuously differentiable function $V: [t_0,\infty)\times\mathbb{R}^n \to \mathbb{R}$, satisfying $\gamma_1(z) \leq V(t,z) \leq \gamma_2(z)$, $\forall z \in \mathbb{R}^n \setminus \{0\}, \forall t \in [t_0,\infty)$, $\gamma_1(z)$ and $\gamma_2(z)$ be continuous positive definite functions, $V(t,z^*) = 0$ and for $V \neq 0$: $\dot{V} \leq 0, \forall t \geq t_f$ and $\dot{V} \leq \frac{-\vartheta(e^V-1)}{e^V(t_f-t)}, \forall t \in [t_0,t_f)$ for (16), then the equilibrium point of dynamics (16) is PUBST-based stable. This also signifies that $z(t)$ converges to the optimal solution $z^*(t)$ in a priori chosen time.*

Proof. Let us select the Lyapunov function candidate

$$V = \|\nabla\mathcal{F}(t,z)\|^2 \tag{17}$$

The derivative of the V along the dynamics (16) for $t \in [t_0,t_f)$

$$\begin{aligned}\dot{V}(z) &= 2(\nabla\mathcal{F}(t,z))^\top\left(\nabla^2\mathcal{F}(t,z)\dot{z} + \frac{\partial\nabla\mathcal{F}(t,z)}{\partial t}\right)\\ &= 2(\nabla\mathcal{F})^\top\left(-\vartheta\psi - \ell\frac{\nabla\mathcal{F}}{\|\nabla\mathcal{F}\|} + \frac{\partial\nabla\mathcal{F}}{\partial t}\right)\end{aligned}$$

Using Cauchy–Schwarz inequality, we can further write,

$$\leq -2\vartheta\nabla\mathcal{F}^\top\psi - 2\ell\|\nabla\mathcal{F}\| + 2\|\nabla\mathcal{F}\|\left\|\frac{\partial\nabla\mathcal{F}}{\partial t}\right\|$$

Since, $\left\|\frac{\partial\nabla\mathcal{F}}{\partial t}\right\| \leq \ell$, then further we get,

$$\dot{\mathcal{V}}(z) \leq -2\vartheta\nabla\mathcal{F}^\top\psi$$

The above inequality is similar to inequality (12). Then proceeding in a similar way as in the proof of Theorem 1, we get inequality (15) which represents PUBST-based stability, implying the trajectory of (16) converges to the optimal solution of $\mathcal{F}(t,z)$ in a priori chosen time. Next for $t > t_f$, proceeding in a similar way as for $t \in [t_0,t_f)$, we get $\dot{\mathcal{V}} \leq 2\vartheta\mathcal{V}$, hence trajectories of (16) will maintain $z^*(t)$. Hence, the equilibrium point of system (16) is PUBST-based stable. □

Computational Cost: We can discuss the convergence rates of Euler discretization to calculate complexity considering the assumption of Lipschitz smoothness. Let us consider the Euler discretized version of the proposed Robust Newton-like method for PUBSTC-TVO dynamics (16). To simplify the computation of complexity, we can write $\psi(t,z) = \frac{\nabla\mathcal{F}(t,z)}{t_f-t}$. Let, $\mathfrak{K} = t_f/h$. Hence, the considered discretized version of the proposed dynamics, taking h as practical step size, can be written as:

$$z(k+1) = \begin{cases} z(k) - h\left(\frac{\vartheta}{\mathfrak{K}-k} + \frac{\ell}{\|\mathcal{F}(k,z)\|}\right)(\nabla^2\mathcal{F}(k,z))^{-1}\\ \quad\nabla\mathcal{F}(k,z) \text{ for } 0 \leq k < \mathfrak{K}\\ z(k) - h\left(\vartheta + \frac{\ell}{\|\mathcal{F}(k,z)\|}\right)(\nabla^2\mathcal{F}(k,z))^{-1}\\ \quad\nabla\mathcal{F}(k,z) \text{ for } \mathfrak{K} \leq k < \infty\end{cases} \tag{18}$$

Let, $\gamma_{1k} := \left(\frac{\vartheta}{\mathfrak{K}-k} + \frac{\ell}{\|\mathcal{F}(k,z)\|}\right)$, and $\gamma_{2k} := \left(\vartheta + \frac{\ell}{\|\mathcal{F}(k,z)\|}\right)$ and $\gamma_{1k}, \gamma_{2k} \in \mathbb{R}_{>0}$.

We need to introduce an extra assumption of L-Lipschitz smooth, as given below:

Assumption (Lipschitz Smoothness of Order q). We assume the function $\mathcal{F}$ is L-Lipschitz smooth of order $q \in (1,2]$, that is, for any $z, y \in \mathbb{R}^n$,

$$\|\nabla\mathcal{F}(k,y) - \nabla\mathcal{F}(k,z)\| \leq L\|y-z\|^{q-1} \tag{19}$$

The smoothness assumption is a prevalent setting in optimization algorithm literature. This assumption is also called (L,q) Holder continuity, it will lead to the following property:

$$\mathcal{F}(k,y) \leq \mathcal{F}(k,z) + \langle\nabla\mathcal{F}(k,z), y-z\rangle + \frac{L}{q}\|y-z\|^q \tag{20}$$

When $q = 2$, the function will be Lipschitz smooth.

10991514, 2025, 4, Downloaded from https://onlinelibrary.wiley.com/doi/10.1002/oca.3292 by Indian Institute Of Technology, Wiley Online Library on [05/06/2026]. See the Terms and Conditions (https://onlinelibrary.wiley.com/terms-and-conditions) on Wiley Online Library for rules of use; OA articles are governed by the applicable Creative Commons License

Considering the following assumptions, for our case, we can calculate iteration complexity as follows:

$$\begin{aligned}&\mathcal{F}(k+1, z(k+1))\\&\quad\le \mathcal{F}(k, z(k)) + \langle \nabla\mathcal{F}(k, z(k)), z(k+1) - z(k)\rangle\\&\quad\quad+\frac{L}{q}\|z(k+1)-z(k)\|^q\end{aligned} \tag{21}$$

Using algorithm (18), for $0 \le k < \mathfrak{K}$ and considering the Lipschitz continuity of the gradient and for $q = 2$

$$\begin{aligned}\mathcal{F}(k+1, z(k+1)) &\le \mathcal{F}(k, z(k)) - \frac{\gamma_{1k}h}{L}\|\nabla\mathcal{F}\|^2 + \frac{\gamma_{1k}^2 h^2}{2L}\|\nabla\mathcal{F}\|^2\\&= \mathcal{F}(k, z(k)) - \frac{\gamma_{1k}h}{L}(1-\gamma_{1k}h/2)\|\nabla\mathcal{F}\|^2\end{aligned}$$

Furthermore, using the Assumption 2 (PL inequality):$\|\nabla\mathcal{F}\|^2 \ge \alpha(\mathcal{F}-\mathcal{F}^*)$, where $\alpha > 0$, we can further write

$$\mathcal{F}(k+1, z(k+1)) \le \mathcal{F} - \frac{\gamma_{1k}h\alpha}{L}(1-\gamma_{1k}h/2)(\mathcal{F}-\mathcal{F}^*(k))$$

Subtracting $\mathcal{F}^*$ on both sides and $\kappa := (1 - 0.5h\gamma_{1k})$, then

$$\begin{aligned}&\mathcal{F}(k+1, z(k+1)) - \mathcal{F}^*(k)\\&\quad\le \left(1 - \frac{\gamma_{1k}h\alpha\kappa}{L}\right)(\mathcal{F}(k, z(k)) - \mathcal{F}^*(k))\end{aligned}$$

Then for $\mathfrak{K}$ iterations with a fixed step size h

$$\mathcal{F}(\mathfrak{K}, z(\mathfrak{K})) - \mathcal{F}^*(k) \le \left(1 - \frac{\gamma_{1k}h\alpha\kappa}{L}\right)^{\mathfrak{K}}(\mathcal{F}(0, z(0)) - \mathcal{F}^*(k))$$

By the inequality, $e^{-z} \ge 1 - z$ we can get that the corresponding iteration complexity is $\mathcal{O}\left(\left(\frac{\gamma_{1k}h\alpha\kappa}{L}\right)^{-1}\ln\frac{1}{\epsilon}\right)$ for ϵ-closeness of $z(k)$ to $z^*(k)$. Similarly, if we run the algorithm for K iterations then for $\mathfrak{K} \le k < K$, the corresponding iteration complexity is $\mathcal{O}\left(\left(\frac{\gamma_{2k}h\alpha\kappa}{L}\right)^{-1}\ln\frac{1}{\epsilon}\right)$.

4.1.3 | Levenberg–Marquardt-Like PUBSTC-TVO Without Invertible Hessian

Let inverse of $\nabla^2\mathcal{F}$ is singular or near singular then the Newton-like technique is not well defined. Suppose $(\nabla^2\mathcal{F} + \wp I_n)$ is invertible for some damping factor $\wp > 0$ then in order to track $z^*(t)$ of (8) in PUBST, we propose the following dynamics:

$$\dot{z}(t) = \begin{cases} -(\nabla^2\mathcal{F}(t,z) + \wp I_n)^{-1}\left(\vartheta\psi(t,z) + \frac{\partial\nabla\mathcal{F}(t,z)}{\partial t}\right) \\ \quad \text{for } t_0 \le t < t_f \\ -(\nabla^2\mathcal{F}(t,z) + \wp I_n)^{-1}\left(\vartheta\nabla\mathcal{F}(t,z) + \frac{\partial\nabla\mathcal{F}(t,z)}{\partial t}\right) \\ \quad \text{for } t \ge t_f \end{cases} \tag{22}$$

where $z(t) \in \mathbb{R}^n$, $\vartheta, \wp \in \mathbb{R}$ and satisfies $\vartheta > 1$, $\psi(t,z) = (\psi_1, \psi_2, \dots, \psi_n) \in \mathbb{R}^{n\times 1}$, $\psi_i = \frac{(e^{\nabla\mathcal{F}_{z_i}(t,z)}-1)}{e^{\nabla\mathcal{F}_{z_i}(t,z)}(t_f - t)}$, for $1 \le i \le n$ and consider the dynamics (22) as a perturbed version of (10) with input $\wp$.

Remark 8. One of the methods for calculating the damping factor at a particular instant includes taking the negative of the minimum eigenvalue of the Hessian matrix at that instant.

Theorem 3. *Consider the dynamics (22). Suppose that $\mathcal{F} : \mathbb{R}_{\ge 0} \times \mathbb{R}^n \to \mathbb{R}$ in (8) satisfies Assumption 1 and Assumption 2 with $p = 1/2$ and $\exists$ a PUBST-ISS Lyapunov function $V : [t_0, \infty) \times \mathbb{R}^n \to \mathbb{R}$ for (22) then dynamics (22) is PUBST-ISS.*

Proof. Let us select the Lyapunov function candidate

$$V = \|\nabla\mathcal{F}(t,z)\|^2 + 2\wp(\mathcal{F}(t,z) - \mathcal{F}^*(t)) \tag{23}$$

The derivative of the V along the dynamics (22) gives

$$\begin{aligned}\dot{V} &= 2\nabla\mathcal{F}^\top\left(\nabla^2\mathcal{F}\dot{z} + \frac{\partial\nabla\mathcal{F}}{\partial t}\right) + 2\wp\nabla\mathcal{F}^\top\dot{z} - 2\wp\dot{\mathcal{F}}^*\\&= 2\nabla\mathcal{F}^\top\big((\nabla^2\mathcal{F} + \wp I_n)\big(-(\nabla^2\mathcal{F} + \wp I_n)^{-1}\\&\quad\times\left(\vartheta\psi(t,z) + \frac{\partial\nabla\mathcal{F}}{\partial t}\right)\big) + \frac{\partial\nabla\mathcal{F}}{\partial t}\big) - 2\wp\dot{\mathcal{F}}^*\\&= -2\vartheta(\nabla\mathcal{F}(t,z))^\top\psi(t,z) - 2\wp\dot{\mathcal{F}}^*\end{aligned} \tag{24}$$

Taking the worst case, we assume $\sup_{t\ge 0}(\dot{\mathcal{F}}^*(t)) < -a$, $a \in \mathbb{R}_{>0}$, then further we can write,

$$\dot{V} \le -2\vartheta\frac{|\nabla\mathcal{F}_{z_i}(t,z)|(e^{|\nabla\mathcal{F}_{z_i}(t,z)|}-1)}{e^{|\nabla\mathcal{F}_{z_i}(t,z)|}(t_f - t)} + 2a\wp, \quad \text{for any i} \tag{25}$$

Next, using PL inequality with $p = 1/2$, we get $V \le \left(1 + \frac{2\wp}{w}\right)\|\nabla\mathcal{F}\|^2$. Since, $V \le n(1 + (2\wp/w))(\max\{|\nabla\mathcal{F}_1|, |\nabla\mathcal{F}_2|, \dots, |\nabla\mathcal{F}_n|\}^2)$ We assume that at a particular time, $\max\{|\nabla\mathcal{F}_1|, |\nabla\mathcal{F}_2|, \dots, \|\nabla\mathcal{F}_n|\}$ returns $|\nabla\mathcal{F}_i|$ and $n(1 + (2\wp/w)) = c$ then, $\sqrt{V/c} \le |\nabla\mathcal{F}_i|$. Using this fact in (25) gives, $\dot{V} \le -2\vartheta\frac{\sqrt{V/c}(e^{\sqrt{V/c}}-1)}{e^{\sqrt{V/c}}(t_f - t)} + 2a\wp$. Next, let $\hat{V} = \sqrt{V/c}$, hence, $\dot{\hat{V}} = \frac{\dot{V}}{2c\hat{V}}$, Further

$$\dot{\hat{V}} \le -\frac{\hat{\vartheta}(e^{\hat{V}} - 1)}{e^{\hat{V}}(t_f - t)} + \gamma(|\wp|) \tag{26}$$

where γ is a class $\mathcal{K}$ function and suppose $\hat{\vartheta} = \frac{\vartheta}{c} > 1$. Next, for $t > t_f$, after equation (24) along the dynamics (22) proceeding in the similar way as for $t \in [t_0, t_f)$, we get $\dot{V} \le -2\vartheta V + \gamma(|\wp|)$ and combining it with (26), we get $\dot{V} \le -\beta(\|z_0\|, t_f - t) - \alpha(\|z\|) + \gamma(\|\wp\|)$, where β is $\mathcal{KL}$ class function and α, γ are the class $\mathcal{K}$ functions. Hence, $V(t,z)$ satisfies the PUBST-ISS Lyapunov function condition thus from Lemma 2, system (22) is PUBST-ISS. □

Remark 9. The damping term $\wp$ functions as a regularizer, ensuring that $(\nabla^2\mathcal{F}(t,z) + \wp I_n)$ remains positive definite even when the Hessian is singular, thereby guaranteeing its invertibility. The adaptive nature of $\wp$ influences the algorithm's behavior: $\wp$ is large (when the Hessian is singular), then the algorithm resembles a Gradient-like PUBSTC-TVO algorithm:

$$\dot{z}(t) = \begin{cases} -(\wp I_n)^{-1}\left(\vartheta\psi(t,z) + \frac{\partial\nabla\mathcal{F}(t,z)}{\partial t}\right), & \text{for } t_0 \le t < t_f \\ -(\wp I_n)^{-1}\left(\vartheta\nabla\mathcal{F}(t,z) + \frac{\partial\nabla\mathcal{F}(t,z)}{\partial t}\right), & \text{for } t \ge t_f, \end{cases}$$

whereas $\wp$ is small (when the Hessian is well-conditioned), the algorithm exhibits behavior similar to the proposed Newton-like PUBSTC-TVO algorithm (10).

10991514, 2025, 4, Downloaded from https://onlinelibrary.wiley.com/doi/10.1002/oca.3292 by Indian Institute Of Technology, Wiley Online Library on [05/06/2026]. See the Terms and Conditions (https://onlinelibrary.wiley.com/terms-and-conditions) on Wiley Online Library for rules of use; OA articles are governed by the applicable Creative Commons License

4.2 | Time-Varying Constrained Convex Optimization

In this subsection, we extend the results of Section 4.1 for constrained TVO problems with inequality constraints.

4.2.1 | PUBSTC-TVO With Inequality Constraints

Consider the constrained TVO problem

$$\begin{aligned} z^*(t) &:= \underset{z\in\mathbb{R}^n}{\operatorname{argmin}}\ \mathcal{F}(t,z) \\ \text{s.t.} \quad & g_i(t,z) \le 0, \quad i \in \{1,2,\dots,r\} \end{aligned} \tag{27}$$

where $g = [g_1, g_2, \dots, g_r]^\top$ with all g_i being convex functions in $z \in \mathbb{R}^n$, $\forall t \ge 0$ and fulfills Assumptions 1–3 and 4.

To include the constraints in the objective function, we introduce a vector of Lagrange multipliers $\lambda \in \mathbb{R}^r_{\ge 0}$ and $\mathcal{L} : \mathbb{R}_{\ge 0} \times \mathbb{R}^n \times \mathbb{R}^r_{\ge 0} \to \mathbb{R}$ associated with TVO in (27) is

$$\mathcal{L}(t,z,\lambda) := \mathcal{F}(t,z) + \sum_{i=1}^{r} \lambda_i g_i(t,z) \tag{28}$$

The dual function is $\mathfrak{T}^*(t) := \arg\max_{\lambda\in\mathbb{R}^r} \mathfrak{G}(t,\lambda)$, where $\mathfrak{G}(t,\lambda) := \min_{z\in\mathbb{R}^n} \mathcal{L}(t,z,\lambda)$. The necessary and sufficient KKT conditions [21] for optimality under Assumptions 1 3 and 4, $\forall t \ge 0$ are

$$\nabla\mathcal{F}(t,z^*) + \sum_{i=1}^{r} \lambda_i^* \nabla g_i(t,z^*) = 0 \tag{29}$$

$$\lambda_i^* g_i(t,z^*) = 0 \tag{30}$$

$$\lambda_i^* \ge 0 \tag{31}$$

$$g_i(t,z^*) \le 0, \quad \forall i \in \{1,2,\dots,r\} \tag{32}$$

Next, we formulate perturbed KKT conditions, where we modify (30) as $\lambda_i^* g_i(t,\hat{z}^*) = -\frac{1}{\sigma} \Rightarrow \lambda_i^* = -\frac{1}{\sigma g_i(t,\hat{z}^*)}$, where $\sigma : \mathbb{R}_{\ge 0} \to \mathbb{R}_{>0}$ is defined as a barrier parameter and $\sigma \to 0$ as $\hat{z}(t) \to z^*(t)$. Next, upon substituting the obtained λ_i^* from perturbed KKT condition in (29), we get

$$\nabla(\mathcal{F}(t,\hat{z}^*) - \frac{1}{\sigma}\sum_{i=1}^{r} \log(-g_i(t,z^*)) = 0 \tag{33}$$

which also satisfies KKT conditions (31) and (32). Next, we define the approximate optimal trajectory and Lagrangian $\mathcal{L} : \mathbb{R}_{\ge 0} \times \mathbb{R}^n \times \mathbb{R}_{>0} \times \mathbb{R}_{\ge 0} \to \mathbb{R}$ associated with (27) using $\sigma(t)$ and $\delta(t)$, where $\delta(t) : \mathbb{R}_{\ge 0} \to \mathbb{R}_{\ge 0}$ is defined as a slack function. It is to be noted that the $\delta(t)$ enlarges the initial feasible set.

$$\begin{aligned} \hat{z}^*(t) &:= \underset{z\in\tilde{D}}{\arg\min}\ \mathcal{F}(t,z) - \frac{1}{\sigma(t)}\sum_{i=1}^{r} \log(\delta(t) - g_i(t,z)) \\ \tilde{\mathcal{L}}(t,z,\sigma,\delta) &:= \mathcal{F}(t,z) - \frac{1}{\sigma(t)}\sum_{i=1}^{r} \log(\delta(t) - g_i(t,z)) \end{aligned} \tag{34}$$

where $z \in \tilde{D}$, $\tilde{D} := \{z \in \mathbb{R}^n : g_i(t,z) < \delta(t), i \in \{1,\dots,r\}\}$ is an open set such that $D \subset \tilde{D}$. In the next lemma, we indicate the approximation error.

Lemma 4 ([8]). *Under the Assumptions 3 and 4 $\forall\ \lambda^* \in \mathfrak{T}^*(t)$ and $t \ge 0$, the following inequality holds*

$$|\mathcal{F}(t,\hat{z}^*) - \mathcal{F}(t,z^*)| \le \frac{r}{\sigma(t)} + \delta(t)\left(\inf_{\lambda^*\in\mathfrak{T}(t)^*} \|\lambda^*\|\right) \tag{35}$$

Remark 10. Lemma 4 says that if $\sigma(t)$ and $\delta(t)$ are chosen so that right-hand side of (35) converges to zero, then the approximate trajectory $\hat{z}^*(t)$ converges to $z^*(t)$.

To track the optimal solution $\hat{z}^*(t)$ in PUBST, we aim to design a dynamics so that gradient of $\tilde{\mathcal{L}}$ defined in (34) vanishes in predefined time. Consider the following proposed dynamics in terms of Lagrangian (34) as:

$$\dot{z}(t) = \begin{cases} -(\nabla^2\tilde{\mathcal{L}})^{-1}\left(\vartheta\psi(t,z,\sigma,\delta) + \frac{\partial\nabla\tilde{\mathcal{L}}}{\partial\sigma}\dot{\sigma} + \frac{\partial\nabla\tilde{\mathcal{L}}}{\partial\delta}\dot{\delta} + \frac{\partial\nabla\tilde{\mathcal{L}}}{\partial t}\right) \\ \quad \text{for} \quad t_0 \le t < t_f \\ -(\nabla^2\tilde{\mathcal{L}})^{-1}\left(\vartheta\nabla\tilde{\mathcal{L}} + \frac{\partial\nabla\tilde{\mathcal{L}}}{\partial\sigma}\dot{\sigma} + \frac{\partial\nabla\tilde{\mathcal{L}}}{\partial\delta}\dot{\delta} + \frac{\partial\nabla\tilde{\mathcal{L}}}{\partial t}\right) \\ \quad \text{for } t \ge t_f \end{cases} \tag{36}$$

where $\vartheta \in \mathbb{R}$ and satisfies $\vartheta > 1$, $\psi(t,z,\sigma,\delta) = (\psi_1,\psi_2,\dots,\psi_n) \in \mathbb{R}^{n\times 1}$, $\psi_i = \frac{(e^{\nabla\tilde{\mathcal{L}}_{z_i}(t,z,\sigma,\delta)}-1)}{e^{\nabla\tilde{\mathcal{L}}_{z_i}(t,z,\sigma,\delta)}(t_f-t)}$, for $1 \le i \le n$.

Theorem 4. *Consider the dynamics (36). Assume that there exist a continuously differentiable function $V : [t_0,\infty) \times D \to \mathbb{R}_{\ge 0}$ satisfying $\gamma_1(z) \le V(t,z) \le \gamma_2(z)$, $\forall z \in D \setminus \{0\}, \forall t \in [t_0,\infty)$, $\gamma_1(z)$ and $\gamma_2(z)$ be continuous positive definite functions, $V(t,\hat{z}^*) = 0$ and for $V \ne 0$: $\dot{V} \le 0, \forall t \ge t_f$ and $\dot{V} \le \frac{-\vartheta(e^V-1)}{e^V(t_f-t)}, \forall t \in [t_0,t_f)$ for (36), then the equilibrium point of dynamics (36) is PUBST based stable. This also signifies that $z(t)$ converges to the optimal solution $\hat{z}^*(t)$ in a priori chosen time.*

Proof. Let us select the Lyapunov functional candidate

$$V = \|\nabla\tilde{\mathcal{L}}(t,z,\sigma,\delta)\|^2, \tag{37}$$

The derivative of the V along the dynamics (10) for $t \in [t_0,t_f)$

$$\begin{aligned} \dot{V}(z) &= 2(\nabla\tilde{\mathcal{L}})^\top\left(\nabla^2\tilde{\mathcal{L}}\dot{z} + \frac{\partial\nabla\tilde{\mathcal{L}}}{\partial\sigma}\dot{\sigma} + \frac{\partial\nabla\tilde{\mathcal{L}}}{\partial\delta}\dot{\delta} + \frac{\partial\nabla\tilde{\mathcal{L}}}{\partial t}\right) \\ &= 2(\nabla\tilde{\mathcal{L}})^\top\left(\nabla^2\tilde{\mathcal{L}}\left(-(\nabla^2\tilde{\mathcal{L}})^{-1}\left(\vartheta\psi + \frac{\partial\nabla\tilde{\mathcal{L}}}{\partial\sigma}\dot{\sigma} + \frac{\partial\nabla\tilde{\mathcal{L}}}{\partial\delta}\dot{\delta} + \frac{\partial\nabla\tilde{\mathcal{L}}}{\partial t}\right)\right)\right. \\ &\quad \left. + \frac{\partial\nabla\tilde{\mathcal{L}}}{\partial\sigma}\dot{\sigma} + \frac{\partial\nabla\tilde{\mathcal{L}}}{\partial\delta}\dot{\delta} + \frac{\partial\nabla\tilde{\mathcal{L}}}{\partial t}\right) \\ &= -2\vartheta(\nabla\tilde{\mathcal{L}})^\top\psi(t,z,\sigma,\delta) \end{aligned} \tag{38}$$

(38) is similar to (12) of convergence analysis performed in Theorem 1. Hence, further analysis can be performed in the same way and finally, we get a similar expression as (15) in Theorem 1,

$$\dot{\hat{V}} \le -\frac{\hat{\vartheta}(e^{\hat{V}}-1)}{e^{\hat{V}}(t_f-t)} \tag{39}$$

10991514, 2025, 4, Downloaded from https://onlinelibrary.wiley.com/doi/10.1002/oca.3292 by Indian Institute Of Technology, Wiley Online Library on [05/06/2026]. See the Terms and Conditions (https://onlinelibrary.wiley.com/terms-and-conditions) on Wiley Online Library for rules of use; OA articles are governed by the applicable Creative Commons License

where $\hat{\vartheta} = \frac{\vartheta}{n} > 1$. Thus, inequality (39) represents PUBST based stability, which means the trajectory of (36) converges to the optimal solution of $\mathcal{F}(t,z)$ in a priori chosen predefined-time.

Next, convergence analysis for system (36) for $t \geq t_f$ is similar to Theorem 1 and we get,

$$\begin{aligned}\dot{V}(z) &= 2(\nabla\tilde{\mathcal{L}})^\top\left(\nabla^2\tilde{\mathcal{L}}\dot{z} + \frac{\partial\nabla\tilde{\mathcal{L}}}{\partial\sigma}\dot{\sigma} + \frac{\partial\nabla\tilde{\mathcal{L}}}{\partial\delta}\dot{\delta} + \frac{\partial\nabla\tilde{\mathcal{L}}}{\partial t}\right)\\ &= -2\vartheta(\nabla\tilde{\mathcal{L}}(t,z,\sigma,\delta))^\top\nabla\tilde{\mathcal{L}}(t,z,\sigma,\delta)\\ &= -2\vartheta V\end{aligned}$$

So, for $t \geq t_f$, the equilibrium point of system (36) is asymptotically stable, therefore trajectories of (36) will remain optimal. Hence, the equilibrium point of system (36) is PUBST-based stable. □

5 | Illustrative Examples

This section provides three simulation examples to illustrate the PUBST-based stability for the continuous-time dynamics proposed in this note. Euler discretization is used for MATLAB implementation with a constant time step size of Δt. Here, the convergence time (t_{ac}) in seconds is equal to $t_{ac}/\Delta t$ iterations.

5.1 | Numerical Examples

Example 1. Minimize

$$\frac{1}{2}\begin{bmatrix} z_1 - \cos(t) \\ z_2 - \sin(t)\end{bmatrix}^\top \begin{bmatrix} 3-2\cos(2t) & 2\sin(2t) \\ 2\sin(2t) & 3+2\cos(2t)\end{bmatrix}\begin{bmatrix} z_1 - \cos(t) \\ z_2 - \sin(t)\end{bmatrix}$$

First, we implemented PUBST-based proposed dynamics (10) using the forward Euler discretization method in MATLAB to solve the above TVO problem.

The initial conditions are $z_0 = [-2\ 0]^\top$. Figure 1a shows that the norm of the gradient of objective function vanishes in predefined-time 0.6 s and the comparison of the result with fixed-time convergent (FxTC) algorithm discussed in Hong et al. [9] is also shown. Figure 1b shows the evolution of states which starts tracking the optimal trajectory $z^*(t)$ in time $t_f = 0.6$ s, which is chosen a priori. In Figure 2, we plot $\|\mathcal{F}(t,z)\|$ versus t for different sampling periods $\Delta t \in \{10^{-2}, 10^{-3}, 10^{-4}\}$. We notice that steady-state error increases as we increase Δt. The log scale is used on the y axis such that the variation of $\|\nabla\mathcal{F}\|$ for values near zero is clearly shown.

Next, we show the comparison results with the prediction-correction method based on standard Newton flow dynamics presented in Fazlyab et al. [8] as: $\dot{z}(t) = -(\nabla^2\mathcal{F}(t,z))^{-1}\left(\vartheta\nabla\mathcal{F}(t,z) + \frac{\partial\nabla\mathcal{F}(t,z)}{\partial t}\right)$. It is shown in Figure 3a that with the same initial condition $z_0 = [-2\ 0]^\top$ and $\vartheta = 5$, $\|\nabla\mathcal{F}\|$ vanishes within predefined time $t_f = 0.3$ s using proposed dynamics (10) and using standard Newton flow dynamics discussed in Fazlyab et al. [8], $\|\nabla\mathcal{F}\|$ takes more than $t = 1.2$ s in reaching zero. In Figure 3b, it's shown that z_1, z_2 calculated using proposed dynamics (10) starts tracking optimal trajectory within predefined time $t_f = 0.3$ s while using standard Newton Flow dynamics, optimal trajectory tracking starts after $t = 1.2$ s.

Next, we solved the above example using a robust dynamics proposed in (16). We took initial conditions as $z_0 = [-2\ 0]^\top$, $t_f = 0.6$ s, $\ell = 2$, $\vartheta = 5$. Figure 4a shows that the norm of the gradient of the objective function vanishes in predefined-time 0.6 s. In Figure 4b, log scale is used on the y axis such that the variation of $\|\nabla\mathcal{F}\|$ for values near zero is clearly shown. Furthermore, we show the comparison results from Newton flow robust dynamics for solving TVO problems: $\dot{z}(t) = -(\nabla^2\mathcal{F}(t,z))^{-1}\left(\vartheta\nabla\mathcal{F}(t,z) + \ell\frac{\nabla\mathcal{F}(t,z)}{\|\nabla\mathcal{F}(t,z)\|}\right)$. It is shown in Figure 5a

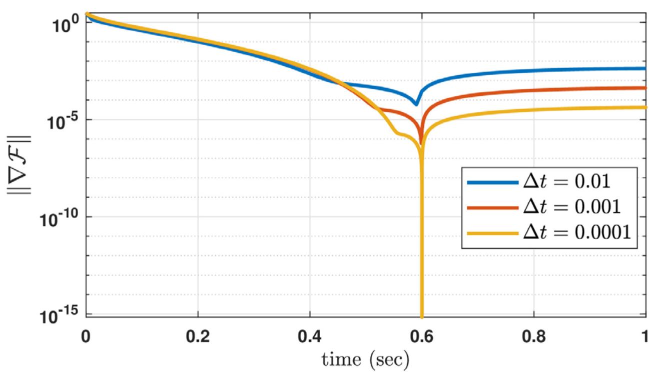

FIGURE 2 | Plot of $\|\nabla\mathcal{F}(t,z(t))\|$ on semilog scale, where $z(t)$ is the solution to the discretized version of dynamics (10) with time for various step sizes (Δt).

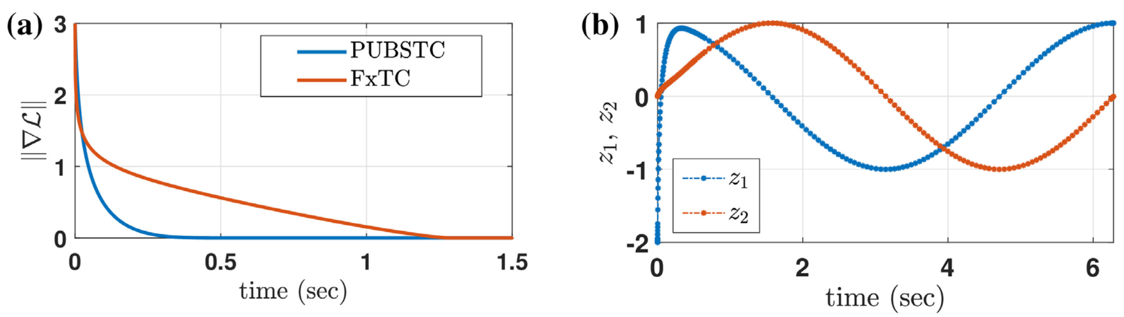

FIGURE 1 | Results using PUBSTC-TVO dynamics (10) in solving Example 1. (a) Comparison between $\|\nabla\mathcal{F}\|$ with PUBSTC-TVO with $t_f = 0.6$ s and FxTC in [9]. (b) Evolution of states using dynamics (10) for example 1 based on TVO problem with unconstrained case.

1099154, 2025, 4, Downloaded from https://onlinelibrary.wiley.com/doi/10.1002/oca.3292 by Indian Institute Of Technology, Wiley Online Library on [05/06/2026]. See the Terms and Conditions (https://onlinelibrary.wiley.com/terms-and-conditions) on Wiley Online Library for rules of use; OA articles are governed by the applicable Creative Commons License

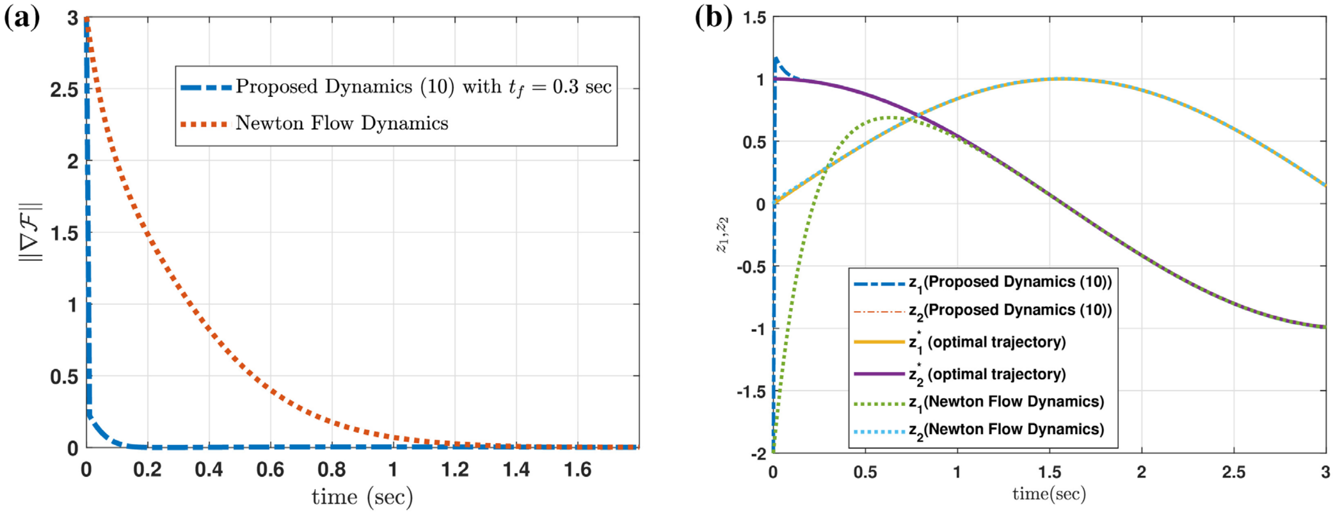

FIGURE 3 | Comparison of results using PUBSTC-TVO dynamics (10) and standard Newton flow dynamics in Fazlyab et al. [8] in solving Example 1. (a) Comparison between $||\nabla\mathcal{F}||$ with PUBSTC-TVO with $t_f = 0.3$ s and standard Newton flow dynamics in Fazlyab et al. [8]. (b) Comparison of the evolution of states using dynamics (10) and standard Newton flow dynamics in Fazlyab et al. [8] for Example 1.

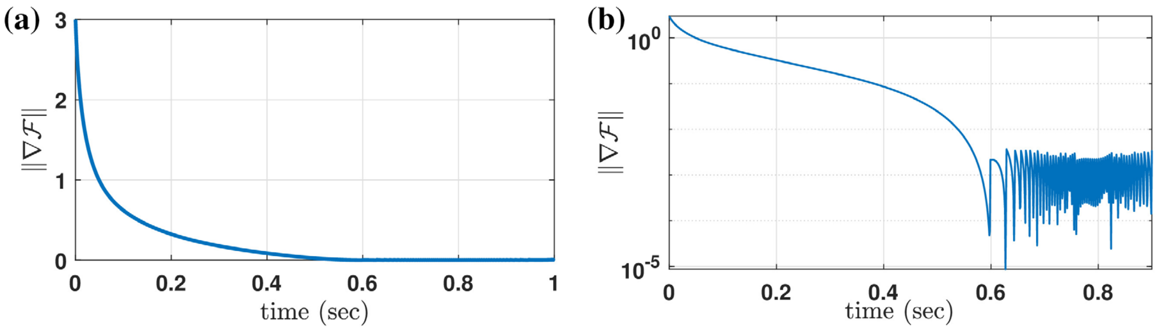

FIGURE 4 | Results using PUBSTC-TVO dynamics (16) in solving Example 1. (a) Plot of $||\nabla\mathcal{F}||$ showing PUBST based convergence within $t_f = 0.6$ s using dynamics (16) for Example 1 of unconstrained case. (b) Plot of $||\nabla\mathcal{F}(t, z(t))||$ on semilog scale where $z(t)$ is the solution to the discretized version of (16) with sampling time $\Delta t = 0.001$ s.

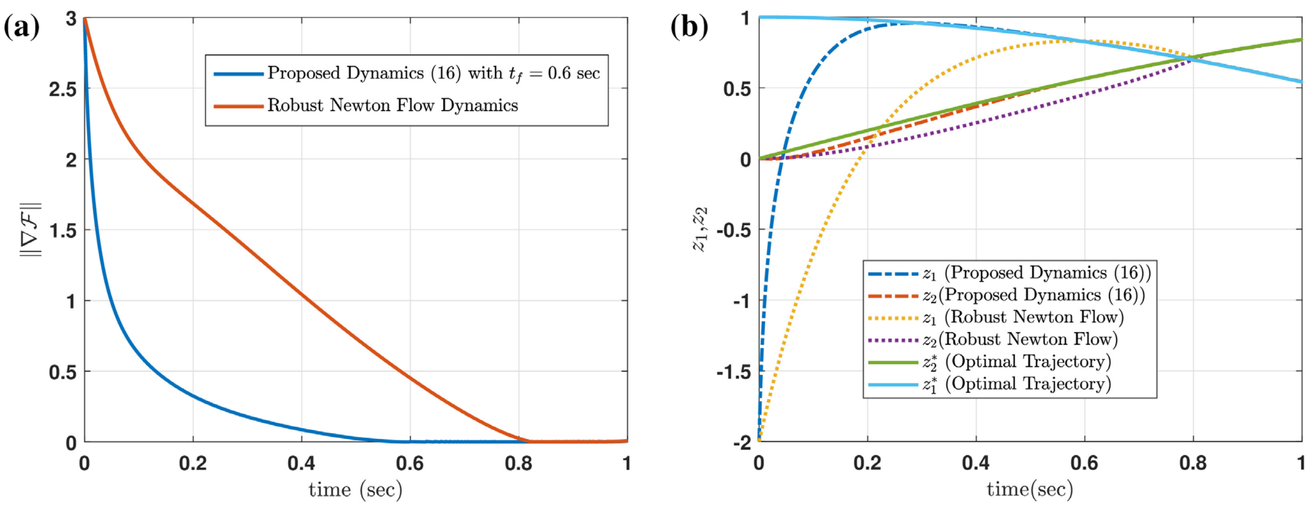

FIGURE 5 | Comparison of results using PUBSTC-TVO dynamics (16) and standard robust Newton flow dynamics in solving Example 1. (a) Comparison showing Plot of $||\nabla\mathcal{F}||$ with PUBST based convergence within $t_f = 0.6$ s using dynamics (16) and standard robust Newton flow dynamics for Example 1 of unconstrained case. (b) Comparison of the evolution of states using dynamics (16) and standard robust Newton flow dynamics for Example 1.

10991514, 2025, 4, Downloaded from https://onlinelibrary.wiley.com/doi/10.1002/oca.3292 by Indian Institute Of Technology, Wiley Online Library on [05/06/2026]. See the Terms and Conditions (https://onlinelibrary.wiley.com/terms-and-conditions) on Wiley Online Library for rules of use; OA articles are governed by the applicable Creative Commons License

that with the same initial condition $z_0 = [-2\ 0]^{\top}$, $t_f = 0.6$ s, $\ell = 2$, $\vartheta = 5$, $\|\nabla\mathcal{F}\|$ vanishes within predefined time $t_f = 0.6$ s using proposed dynamics (16) and using standard robust Newton flow dynamics, $\|\nabla\mathcal{F}\|$ takes more than $t = 0.8$ s in reaching zero. In Figure 5b, it shown that z_1, z_2 calculated using proposed dynamics (16) starts tracking optimal trajectory within predefined time $t_f = 0.6$ s while using standard robust Newton Flow dynamics, optimal trajectory tracking starts after $t = 0.8$ s.

Example 2. Consider the following quadratic TVO problem with ill-conditioned Hessian

$$\text{minimize} \quad (tz - \sin(t))^2 \tag{40}$$

Since, for this example, Hessian will be ill-conditioned, when t is small. Therefore, we apply the proposed Levenberg–Marquardt-like PUBSTC-TVO algorithm (22) to find an optimal trajectory in a prior chosen time. It is important to choose $\wp$ properly. Here, we chose $\wp = e^{-2t}$. The initial condition is $z(0) = 2$, $t_f = 0.5$ s.

It is shown in Figure 6 that the state trajectory obtained by using proposed dynamics (22) starts tracking the optimal trajectory within chosen $t_f \leq 0.5$ s.

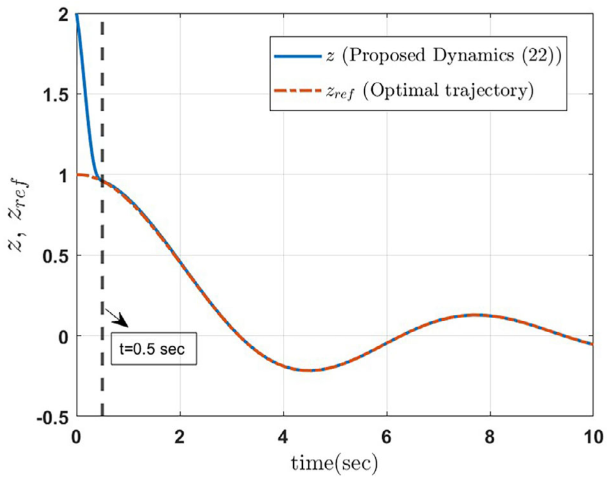

FIGURE 6 | Evolution of state using dynamics (22) for example (40) with ill-conditioned Hessian, and it is shown that it starts tracking optimal trajectory within $t_f = 0.5$ s.

Example 3. Consider the following quadratic TVO problem with inequality constraints:

$$\begin{aligned} \text{minimize} \quad & 0.5(z_1 + \sin(t))^2 + 1.5(z_2 + \cos(t))^2 \\ \text{s.t.} \quad & z_2 - z_1 - \cos(t) \leq 0 \end{aligned} \tag{41}$$

Above example is an illustration of (27), so (34) is written as

$$\begin{aligned} \mathcal{L}(t, z, \sigma, \delta) = {} & 0.5(z_1 + \sin(t))^2 + 0.5(z_2 + \cos(t))^2 \\ & - \frac{1}{\sigma(t)} \log(\delta(t) - (z_2 - z_1 - \cos(t))) \end{aligned} \tag{42}$$

where $\sigma(t) = 10\exp(1000 * t)$, $\delta(t) = 2\exp(-5t)$. We solved it using PUBST-based proposed dynamics (36) with the help of forward Euler's method with constant step size in MATLAB. The initial condition is $z_0 = [-2\ 0]^{\top}$. In Figure 7a, the norm of the gradient of $\nabla\mathcal{L}$ in (42) goes to zero within a priori chosen time of $t_f = 0.1$ s, which is the optimality condition in order to track the optimal trajectory and the comparison of the result with fixed-time convergent (FxTC) algorithm discussed in Hong et al. [9] is also shown. In Figure 7b, the evolution of time-varying states is also shown which follow their optimal trajectory as $\|\nabla\mathcal{L}(t, z(t))\|$ vanishes within predefined-time $t_f = 0.1$ s. In Figure 8, we plot $\|\nabla\mathcal{L}(t, z)\|$ versus t for different $\Delta(t) \in \{10^{-2}, 10^{-3}, 10^{-4}\}$. We notice that steady-state error increases as we increase Δt.

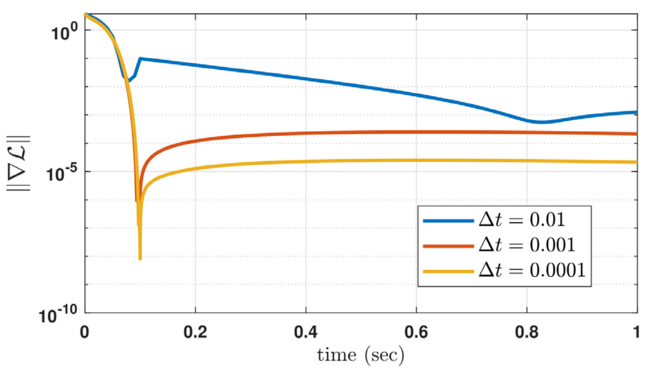

FIGURE 8 | Plot of $\|\nabla\mathcal{L}(t, z(t))\|$ on semilog scale, where $z(t)$ is the solution to the discretized version of dynamics (36) with time for various step sizes (Δt).

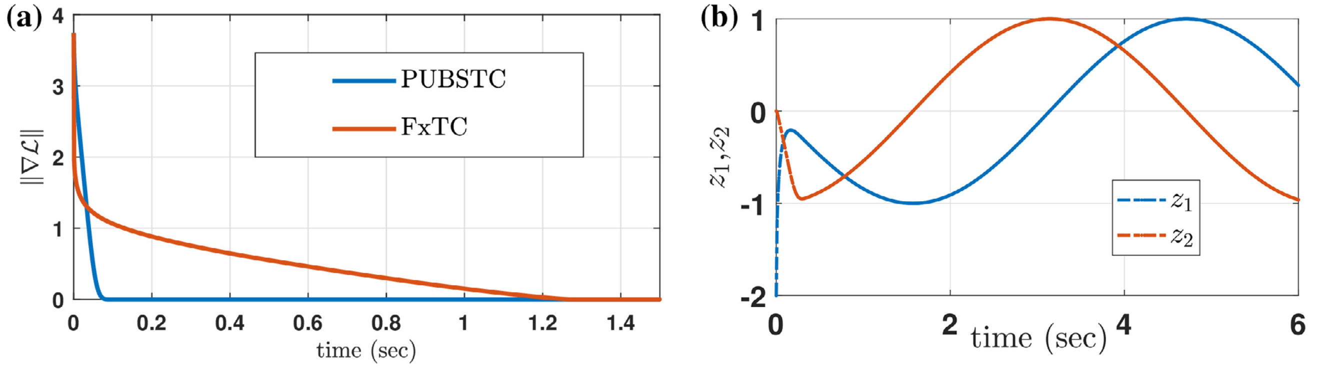

FIGURE 7 | Results using PUBSTC-TVO dynamics (36) in solving Example 2. (a) Comparison between $\|\nabla\mathcal{L}\|$ with PUBST based convergence within $t_f = 0.1$ s and FxTC. (b) Evolution of states for example based on TVO problem with inequality constraints.

10991514, 2025, 4, Downloaded from https://onlinelibrary.wiley.com/doi/10.1002/oca.3292 by Indian Institute Of Technology, Wiley Online Library on [05/06/2026]. See the Terms and Conditions (https://onlinelibrary.wiley.com/terms-and-conditions) on Wiley Online Library for rules of use; OA articles are governed by the applicable Creative Commons License

5.2 | Robot Navigation With Collision Avoidance

In this subsection, we frame the navigation problem as a TVO problem, which can be addressed using the methods developed in this paper. We consider a disk-shaped robot centered at $z \in \mathcal{S}$ with radius $r \in \mathbb{R}_{\geq 0}$ working in a closed compact convex environment $\mathcal{S} \subset \mathbb{R}^n$. Let workspace $\mathcal{S}$ is populated with $m \in \mathbb{Z}_{\geq 0}$ disk-shaped obstacles centered at $z_i \in \mathcal{S}$ with radius $r_i > 0$ for $i \in \{1, 2, \ldots, m\}$. Free space of robot is $\mathcal{F} := \{z \in \mathcal{S} | \overline{\mathcal{B}}(z, r) \subseteq \mathcal{S} \setminus \bigcup_{i=1}^{m} \mathcal{B}(z_i, r_i)\}$, where $\mathcal{B}(z, r)$ represents a n dimensional open ball centered at z with radius r, and $\overline{\mathcal{B}}(z, r)$ represents its closure. Let z_c be the center of mass of the robot and our objective is for $z_c(t)$ to track a moving target $z_d(t) \in \mathcal{F}$ after a certain time $t > 0$ ensuring collision avoidance. Arslan and Koditschek [23], proposed the idea of a projected goal which constitutes a continuous computation of projection of $z_d(t)$ onto a safe neighborhood around z_c. Next, collision-free space around z_c is defined as [23]: $\mathcal{LS}(z_c) := \{z \in \mathcal{S} | c_i(z_c)^\top z - d_i(z_c) \leq 0, i = 1, \ldots, m\}$, where $c_i(z_c) = z_i - z_c$, $d_i(z_c) = (z_i - z_c)^\top \left(\eta_i z_i + (1 - \eta_i) z_c + r \frac{z_c - z_i}{\|z_c - z_i\|}\right)$, where $\eta_i = \frac{1}{2} - \frac{r_i^2 - r^2}{\|z_i - z_c\|^2}$. Assuming the robot follows single integrator dynamics $\dot{z}_c = u(z_c)$, the controller proposed by Arslan and Koditschek [23] is $\dot{z}_c = -k(z_c - \hat{z})$, where $k > 0$ is gain and $\hat{z}$ is the orthogonal projection of z_d onto $\mathcal{LS}(z_c)$. The proposed controller works with the assumption that $\|z_i - z_j\| > r_i + r_j + 2r$.

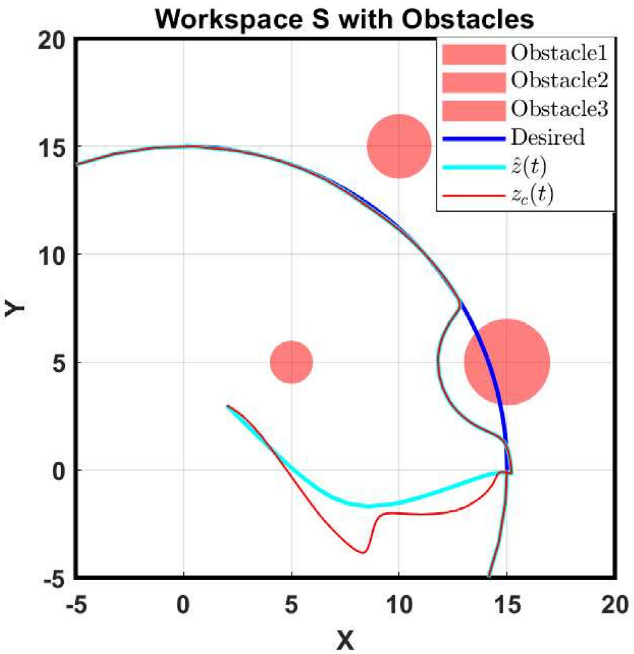

FIGURE 9 | Plot of workspace with three obstacles showing the evolution of desired trajectory $z_d(t)$, estimated projected goal $\hat{z}(t)$, and center of mass of robot $z_c(t)$.

The above problem can be cast as TVO problem discussed in this paper as: $\hat{z} := \arg\min_{z \in \mathbb{R}^n} \frac{1}{2}\|z - z_d(t)\|^2$, s.t. $c_i(z_c)^\top z - d_i(z_c) \leq 0$, $i = 1, \ldots, m$, which is an illustration of (27) so (34) is written as $\tilde{L}(t, z, z_c) = \frac{1}{2}\|z - z_d(t)\|^2 - \frac{1}{\sigma(t)} \sum_{i=1}^{m} \log(d_i(z_c) - c_i(z_c)^\top z)$. We solve the above problem using the proposed continuous-time dynamics (36) and find the estimator $\hat{z}$ of the projection of $z_d(t)$ onto free space $\mathcal{LS}(z_c)$ in a priori chosen time. We propose a controller based on the Lemma 1 to navigate $z_c(t)$ to $\hat{z}(t)$ in a priori chosen time. Controller dynamics is:

$$u = \begin{cases} -k \frac{e^{(z_c(t) - \hat{z}(t))} - 1}{e^{(z_c(t) - \hat{z}(t))}(t_f - t)}, & \text{for } t_0 \leq t < t_f \\ -k(z_c(t) - \hat{z}(t)), & \text{for } t \geq t_f \end{cases} \tag{43}$$

where $k > 1$ is gain.

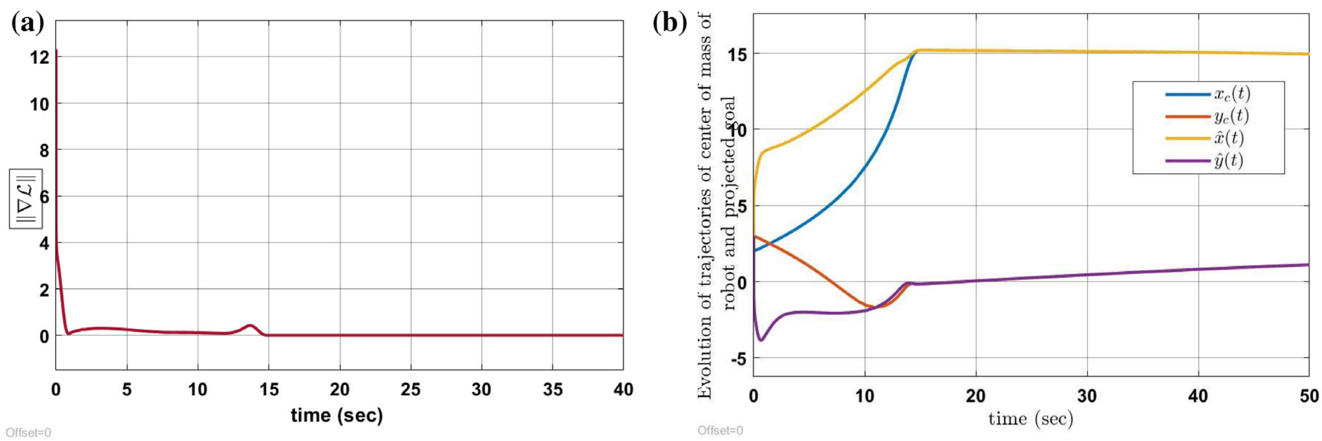

FIGURE 10 | Results using PUBSTC-TVO dynamics (36) in solving TVO problem considered for computing projected goal required for safe robot navigation and controller (43) used to make $z_c(t)$ follow $\hat{z}(t)$ within $t_f = 15$ s. (a) Evolution of $\|\nabla \mathcal{L}\|$ with PUBST based convergence within $t_f = 15$ s using proposed continuous-time dynamics (36). It is shown that $\|\mathcal{L}\| \to 0$ as $t \to t_f$. (b) Evolution of xy position of center of mass of robot $(x_c(t), y_c(t))$ and projected goal $(\hat{x}, \hat{y})$ evaluated solving TVO problem. It is shown that $z_c(t)$ starts tracking $\hat{z}(t)$ within $t_f = 15$ s.

10991514, 2025, 4, Downloaded from https://onlinelibrary.wiley.com/doi/10.1002/oca.3292 by Indian Institute Of Technology, Wiley Online Library on [05/06/2026]. See the Terms and Conditions (https://onlinelibrary.wiley.com/terms-and-conditions) on Wiley Online Library for rules of use; OA articles are governed by the applicable Creative Commons License

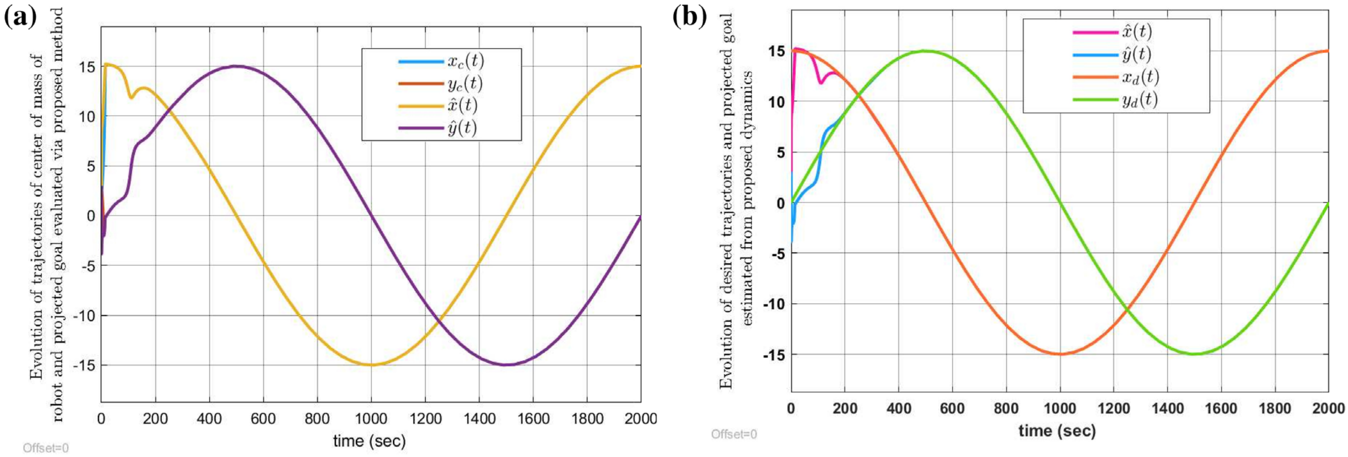

FIGURE 11 | Results using PUBSTC-TVO dynamics (36) in solving TVO problem considered for computing projected goal required for safe robot navigation and plot of the desired trajectory which is moving periodically with $T = 2000$ s. (a) Evolution of xy position of center of mass of robot $(x_c(t), y_c(t))$ and projected goal $(\hat{x}, \hat{y})$ evaluated solving TVO problem for complete time $T = 2000$ s. (b) Evolution of xy position of the desired trajectory $(x_d(t), y_d(t))$ and projected goal $(\hat{x}, \hat{y})$ evaluated solving TVO problem for complete time $T = 2000$ s.

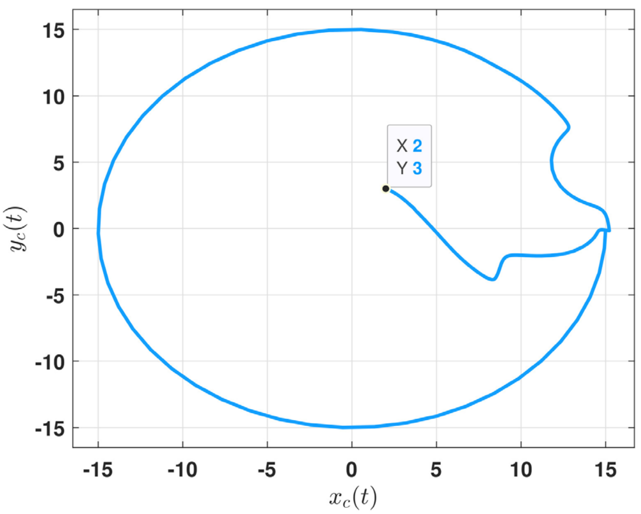

FIGURE 12 | Phase-portrait: $x_c(t)$ opposite $y_c(t)$ showing that center of mass of the robot follows a circular trajectory as desired over time.

In our simulation, we consider a moving target $z_d(t) = [x_d(t), y_d(t)]^\top \in \mathbb{R}^2$, following a circular trajectory with circumference of radius ($r_d = 15$), centered at origin, and moving periodically with $T = 2000$ s. We consider $m = 3$ obstacles in workspace $\mathcal{S}$, with centres $z_1 = [5, 5], z_2 = [15, 5], z_3 = [10, 15]$ with radii $r_1 = 1, r_2 = 2, r_3 = 1.5$, respectively, as shown in Figure 9. We consider a disk-shaped robot with a radius $r = 2$ with the initial point of its center of mass $z_c(0) = [2, 3]$. Next, we solve TVO problem to estimate the projected goal $(\hat{z}(t)) = [\hat{x}(t), \hat{y}(t)]$ using proposed continuous-time dynamics (36), where $\tilde{\mathcal{L}}(t, z, z_c) = \frac{1}{2}\|z - z_d(t)\|^2 - \frac{1}{\sigma(t)}\sum_{i=1}^m \log(d_i(z_c) - c_i(z_c)^\top z)$, here we took $\sigma(t) = e^{0.01t}, \vartheta = 50, t_f = 15$ s. It is shown in Figure 10a that $\|\nabla\mathcal{L}(t, z, z_c)\| \to 0$ as $t \to t_f$, which means we reach estimated optimal trajectory $\hat{z}(t)$ within $t_f = 15$ s. Optimal trajectory $\hat{z}(t)$ provides safe navigation avoiding obstacles in following the desired trajectory which is allowed to intersect obstacles as shown in Figure 9. To track this moving projected target $\hat{z}(t)$ by the robot in a priori chosen time (t_f), we use controller (43), where for simulation, we chose gain $k = 5$. It is shown in Figure 10b that the trajectory of the center of mass of robot $(z_c(t))$ starts tracking $\hat{z}(t)$ within a predefined-time $t_f = 15$ s. Figure 11 shows evolution of trajectories $z_c(t), \hat{z}(t)$, and $z_d(t)$ over time. Figure 12 shows a phase portrait representing navigation of the robot. As we can see in Figure 9, the robot successfully tracks the moving target while avoiding the circular obstacles.

In Figure 13a, we demonstrate that $\|\nabla\tilde{\mathcal{L}}\| \to 0$ within a predefined upper bound of settling time $t_f = 15$ s, whereas dynamics proposed in Fazylab et al. [8] for solving TVO problems with inequality constraints takes more than $t = 40$ s to reach estimated optimal trajectory. Additionally, we show the results obtained by plotting $\|\nabla\tilde{\mathcal{L}}\|$ on a semilog scale. Figure 13b, illustrates that the steady-state error ($\|\nabla\tilde{\mathcal{L}}\| < 10^{-3}$ after $t_f > 15$ s) in the case of proposed dynamics is comparatively much smaller than the Newton flow dynamics. Figure 14 shows the plot of control inputs using dynamics (43) and the controller proposed by Arslan and Koditschek [23]: $\dot{z}_c = -k(z_c - \hat{z})$, where $k > 0$ is gain.

6 | Conclusions

In this note, PUBST-based convergent dynamics are proposed and discussed to solve TVO problems. The proposed method yields a better convergence time compared to the methods available in the literature. Numerical examples and application in robot navigation with collision avoidance show the effectiveness of proposed dynamics. Furthermore, the proposed technique can also be extended for time-varying distributed optimization problems. In addition, one of the motivations behind the study of fast optimization methods is to generate signals for controllers at the same speed as the system evolves.

10991514, 2025, 4, Downloaded from https://onlinelibrary.wiley.com/doi/10.1002/oca.3292 by Indian Institute Of Technology, Wiley Online Library on [05/06/2026]. See the Terms and Conditions (https://onlinelibrary.wiley.com/terms-and-conditions) on Wiley Online Library for rules of use; OA articles are governed by the applicable Creative Commons License

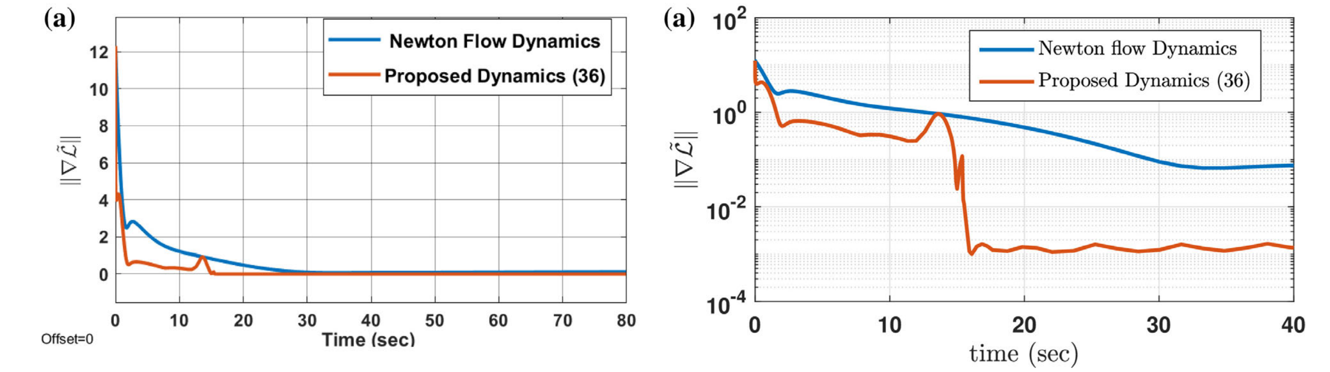

FIGURE 13 | Comparison of results using PUBSTC-TVO dynamics (36) and standard Newton flow dynamics in solving TVO problem considered for computing projected goal required for safe robot navigation. (a) Comparison of evolution of $\|\nabla\tilde{\mathcal{L}}\|$ with PUBST based convergence within $t_f = 15$ s using proposed dynamics (36) and Newton flow dynamics proposed in Fazlyab et al. [8]. (b) Comparison of plot of $\|\nabla\tilde{\mathcal{L}}\|$ on semilog scale between our proposed dynamics (31) to Newton flow dynamics discussed in Fazylab et al. [8] to show the accuracy of proposed dynamics.

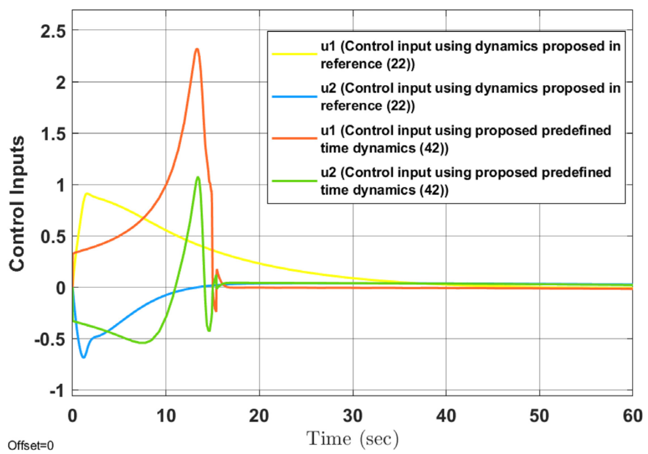

FIGURE 14 | Plot of control inputs using controller dynamics (43) and dynamics proposed in Arslan and Kod [23].

Author Contributions

All authors participated in the theoretical analysis, and manuscript preparation. Each author has read and approved the final manuscript and agrees to be accountable for the work.

Acknowledgments

Sorin Olaru acknowledges the support of the RTE Chair at CentraleSupelec.

Data Availability Statement

The data that support the findings of this study are available from the corresponding author upon reasonable request.

References

1. U. Helmke and J. B. Moore, *Optimization and Dynamical Systems* (Springer Science & Business Media, 2012).

2. W. Su, *Traffic Engineering and Time-Varying Convex Optimization* (Pennsylvania State University, 2009).

3. F. Y. Jakubiec and A. Ribeiro, "Distributed Maximum a Posteriori Probability Estimation of Dynamic Systems With Wireless Sensor Networks," in *2012 IEEE International Conference on Acoustics, Speech and Signal Processing (ICASSP)* (IEEE, 2012), 2857–2860.

4. H. Hong, S. Baldi, W. Yu, and X. Yu, "Distributed Time-Varying Optimization of Second-Order Multiagent Systems Under Limited Interaction Ranges," *IEEE Transactions on Cybernetics* 52, no. 12 (2021): 13874–13886.

5. M. Baumann, C. Lageman, and U. Helmke, "Newton-Type Algorithms for Time-Varying Pose Estimation," in *Proceedings of the 2004 Intelligent Sensors, Sensor Networks and Information Processing Conference* (IEEE, 2004), 155–160.

6. A. Simonetto, A. Mokhtari, A. Koppel, G. Leus, and A. Ribeiro, "A Class of Prediction-Correction Methods for Time-Varying Convex Optimization," *IEEE Transactions on Signal Processing* 64, no. 17 (2016): 4576–4591.

7. S. Rahili and W. Ren, "Distributed Continuous-Time Convex Optimization With Time-Varying Cost Functions," *IEEE Transactions on Automatic Control* 62, no. 4 (2016): 1590–1605.

8. M. Fazlyab, S. Paternain, V. M. Preciado, and A. Ribeiro, "Prediction-Correction Interior-Point Method for Time-Varying Convex Optimization," *IEEE Transactions on Automatic Control* 63, no. 7 (2017): 1973–1986.

9. H. Hong, W. Yu, G. P. Jiang, and H. Wang, "Fixed-Time Algorithms for Time-Varying Convex Optimization," *IEEE Transactions on Circuits and Systems II: Express Briefs* 70, no. 2 (2022): 616–620.

10. S. P. Bhat and D. S. Bernstein, "Finite-Time Stability of Continuous Autonomous Systems," *SIAM Journal on Control and Optimization* 38, no. 3 (2000): 751–766.

11. R. Raveendran, A. D. Mahindrakar, and U. Vaidya, "Dynamical System Approach for Time-Varying Constrained Convex Optimization Problems," *IEEE Transactions on Automatic Control* 69, no. 6 (2023): 3822–3834.

12. D. Gómez-Gutiérrez, "On the Design of Nonautonomous Fixed-Time Controllers With a Predefined Upper Bound of the Settling Time," *International Journal of Robust and Nonlinear Control* 30, no. 10 (2020): 3871–3885.

13. J. D. Sánchez-Torres, D. Gómez-Gutiérrez, E. López, and A. G. Loukianov, "A Class of Predefined-Time Stable Dynamical Systems," *IMA Journal of Mathematical Control and Information* 35, no. Supplement_1 (2018): i1–i29.

14. A. K. Pal, S. Kamal, S. K. Nagar, B. Bandyopadhyay, and L. Fridman, "Design of Controllers With Arbitrary Convergence Time," *Automatica* 112 (2020): 108710.

10991514, 2025, 4, Downloaded from https://onlinelibrary.wiley.com/doi/10.1002/oca.3292 by Indian Institute Of Technology, Wiley Online Library on [05/06/2026]. See the Terms and Conditions (https://onlinelibrary.wiley.com/terms-and-conditions) on Wiley Online Library for rules of use; OA articles are governed by the applicable Creative Commons License

15. P. Prasun, S. Pandey, S. Kamal, S. Ghosh, D. Singh, and D. Ghosh, "Predefined Upper Bound of Settling Time Based Convergent Gradient Flow Systems," in *IECON 2022–48th Annual Conference of the IEEE Industrial Electronics Society* (IEEE, 2022), 1–6.

16. B. Singh, A. K. Pal, S. Kamal, T. N. Dinh, and F. Mazenc, "Vector Control Lyapunov Function Based Stabilization of Nonlinear Systems in Predefined Time," *IEEE Transactions on Automatic Control* 68, no. 8 (2022): 4984–4989.

17. V. K. Singh, S. Kamal, and S. Ghosh, "Prescribed-Time Constrained Feedback Control for an Uncertain Twin Rotor Helicopter," *Aerospace Science and Technology* 140 (2023): 108483.

18. A. F. Filippov, *Differential Equations With Discontinuous Righthand Sides: Control Systems*, vol. 18 (Springer Science & Business Media, 2013).

19. S. Kamal, A. K. Pal, B. Singh, B. Bandyopadhyay, and X. Yu, "Stabilization of Continuous Time Uncertain Systems With Predefined Upper Bound of Settling Time," in *2022 16th International Workshop on Variable Structure Systems (VSS)* (IEEE, 2022), 266–271.

20. H. Karimi, J. Nutini, and M. Schmidt, "Linear Convergence of Gradient and Proximal-Gradient Methods Under the Polyak-łojasiewicz Condition," in *Machine Learning and Knowledge Discovery in Databases: European Conference, ECML PKDD 2016, Riva del Garda, Italy, September 19–23, 2016, Proceedings, Part I 16* (Springer, 2016), 795–811.

21. S. Boyd and L. Vandenberghe, *Convex Optimization* (Cambridge University Press, 2004).

22. A. Hauswirth, Z. He, S. Bolognani, G. Hug, and F. Dörfler, "Optimization Algorithms as Robust Feedback Controllers," *Annual Reviews in Control* 57 (2024): 100941.

23. O. Arslan and D. E. Koditschek, "Exact Robot Navigation Using Power Diagrams," in *2016 IEEE International Conference on Robotics and Automation (ICRA)* (IEEE, 2016), 1–8.

10991514, 2025, 4, Downloaded from https://onlinelibrary.wiley.com/doi/10.1002/oca.3292 by Indian Institute Of Technology, Wiley Online Library on [05/06/2026]. See the Terms and Conditions (https://onlinelibrary.wiley.com/terms-and-conditions) on Wiley Online Library for rules of use; OA articles are governed by the applicable Creative Commons License